ELSEVIER

Contents lists available at ScienceDirect

Zoologischer Anzeiger

journal homepage: www.elsevier.com/locate/jcz



Morphometry of the pedipalp patella provides new characters for species-level taxonomy in whip spiders (Arachnida, Amblypygi): A test case with description of a new species of *Phrynus*



Michael Seiter ^{a, b, *}, Luca Strobl ^a, Thomas Schwaha ^a, Lorenzo Prendini ^c, Frederic D. Schramm ^d

- ^a Department of Evolutionary Biology, Unit Integrative Zoology, University of Vienna, Djerassiplatz 1, 1030, Vienna, Austria
- ^b Naturhistorisches Museum Wien, Burgring 7, 1010, Vienna, Austria
- c Arachnology Lab, Division of Invertebrate Zoology, American Museum of Natural History, Central Park West at 79th Street, New York, NY, 10024-5192, USA
- ^d Worsdell Drive, Gateshead, NE8 2EU, United Kingdom

ARTICLE INFO

Article history: Received 10 April 2021 Received in revised form 20 February 2022 Accepted 21 February 2022 Available online 28 February 2022

Corresponding Editor: Peter Michalik

Keywords:
Systematics
Diagnosis
Morphology
Geometric morphometrics
Cerotegument ultrastructure
Spine variation
Hispaniola

ABSTRACT

Whip spiders (Amblypygi Thorell, 1883) are easily distinguished from their spider relatives (Araneae Clerck, 1757) by their raptorial pedipalps, the second pair of appendages, which are covered in spines and used to grasp and impale prey. Among other characters, the number, distribution, and size differences among the pedipalp spines continue to be important for whip spider systematics at different levels in the taxonomic hierarchy. However, traditional meristic and qualitative characters used to describe the pedipalp spines often limit their use for species-level taxonomy, as character states are invariant or overlapping. The present study employs landmark-based morphometrics to map the morphospace comprising the retrolateral surface of the pedipalp patella and its dorsal spines in a group of Neotropical whip spiders of the genus Phrynus Lamarck, 1801, all of which share an inconspicuous spine on the prodorsal surface of the pedipalp tarsus, i.e., "group B" proposed by Quintero (1983). The analysis presented demonstrates that the relative pedipalp patella lengths and the patella spine P3 length to patella width ratios are of similar use for species diagnosis as the commonly employed relative length of leg femur I. Importantly, the analysis reveals that, beyond the traditional approach of qualitatively reporting relative pedipalp patella dorsal spine lengths (e.g., P3 > P5 > P2 > P4 > P6 > P1), the ratios between spine lengths are useful morphometric characters for species-level taxonomy in Phrynus. New morphometric ratios are provided for the species of *Phrynus* group B and used, together with traditional characters, to describe Phrynus guarionexi sp. nov. from the Dominican Republic. Finally, new morphological data are provided concerning the cerotegument, frontal process and prolateral surface of the pedipalp tibia in the species of group B.

© 2022 Elsevier GmbH. All rights reserved.

1. Introduction

Whip spiders (Amblypygi Thorell, 1883) are a small order of arachnids, currently comprising more than 250 described extant species in 17 genera and five families (Harvey 2003 2013; Miranda et al., 2018 2021). They occur mainly in the tropics and subtropics where their distribution is restricted by their dependence on

E-mail addresses: michael.seiter@univie.ac.at, seitermichael@hotmail.com (M. Seiter).

humidity (Weygoldt 2000). Amblypygi and Uropygi Latreille, 1804 (the group combining Schizomida Petrunkevitch 1945 and Thelyphonida Cambridge 1872) are placed within the clade Pedipalpi Latreille, 1810, and comprise the sister group to true spiders (Araneae Clerck, 1757). Unlike true spiders, Pedipalpi lack venom glands and spinnerets (Shultz 2007; Weygoldt & Paulus 1979). Further, the first pair of legs is not used for locomotion, instead being greatly elongated and sensory in function. Prey is captured and restrained with the highly modified, raptorial pedipalps bearing spines (Weygoldt 2000).

Although the number of studies on whip spiders increased in recent years, their diversity is probably underestimated. Whip

^{*} Corresponding author. Department of Evolutionary Biology, Unit Integrative Zoology, University of Vienna, Djerassiplatz 1, 1030, Vienna, Austria.

spiders are generally perceived as morphologically conservative (e.g., Chirivi-Joya et al., 2020; Seiter & Gredler 2020), a notion supported by genetic data which suggests high levels of genetic divergence within nominal species (Esposito et al., 2015; Reveillion et al., 2020; Schramm et al., 2021). An integrative approach, combining morphology with genetics, behavior and/or karyotype proved successful in delimiting morphologically similar species in several genera (Prendini et al., 2005; Seiter et al., 2020). This approach highlighted the need for new character systems to resolve whip spider taxonomy, a need which is likely to become more pressing with time, as the traditional, narrow set of morphological characters becomes increasingly inadequate for species delimitation and diagnosis with the discovery and description of more diversity.

The morphology of the raptorial pedipalps continues to be important for whip spider systematics at several levels in the taxonomic hierarchy. Interspecific differences in these appendages include meristic characters, e.g., number of spines and tubercles, and qualitative characters, e.g., the presence or absence of particular setae and articulations between pedipalp tarsus and claw. Differences in the relative lengths of pedipalp spines are also important characters for species delimitation. Such characters are usually comparative, with one spine described as being longer or shorter than another (Quintero 1981; 1983; Armas 2006). However, such descriptions do not reflect the range of relative size differences among the pedipalp spines. Furthermore, differences in other characters of the pedipalps, such as their relative proportions, are seldom reported in a manner that permits interspecific comparison, often resulting in similar descriptions for strikingly different pedipalps.

An obvious example is the speciose Neotropical genus *Phrynus* Lamarck, 1801, in which a great variety of pedipalp shapes and relative spine lengths, especially on the femur and patella, contribute to the distinct habitus of each species. Despite their variable appearance, the majority of *Phrynus* exhibit the same number of major dorsal spines on the patella. Furthermore, the fourth spine is shorter than the third and fifth, which are the longest in all species of the genus. As the number of described species of Phrynus and other whip spiders steadily increases, it will become more important to expand the set of characters for comparing their variable pedipalps. Landmark-based morphometrics is a powerful tool for analyzing and comparing the shape of organisms beyond traditional linear measurements but has been little explored in whip spider systematics, thus far. Recent studies demonstrated its utility for tracking the development of sexual dimorphism during postembryonic growth and intraspecific variation (McLean et al., 2018; 2019; Torres et al., 2018; Vásquez et al.,

In the present study, landmark-based morphometrics is used, in addition to other traditional characters, to explore differences in the shape of the retrolateral surface and dorsal spines of the pedipalp patella in a group of *Phrynus* species, all of which share an inconspicuous spine on the prodorsal surface of the pedipalp tarsus. This group was first identified by Quintero (1981) and later termed "group B" in a classification of Phrynus species (Quintero 1983). Group B originally included five species, i.e., Phrynus armasi Quintero, 1981, Phrynus goesii Thorell, 1889, Phrynus longipes (Pocock, 1894), Phrynus pulchripes (Pocock, 1894), and Phrynus tessellatus (Pocock, 1893). Quintero (1981) omitted Phrynus pinarensis Franganillo, 1930 (treated as incertae sedis), which also possesses the distinctive tarsal spine. Phrynus armasi was later synonymized with P. pinarensis by Armas & Avila Calvo (2001), and four new species bearing the tarsal spine were described, i.e., Phrynus araya Colmenares García and Villarreal, 2008, Phrynus calypso Chirivi-Joya, 2017, Phrynus exsul Harvey, 2002, and Phrynus panche Armas and Angarita, 2008, raising the number of species in group B to nine. Except for *P. exsul* which occurs in Indonesia, the species of group B are restricted to the Caribbean archipelago and northern South America.

The morphometric analysis presented herein revealed that relative pedipalp patella lengths, patella spine P3 length to patella width ratios, and the relationship between patella dorsal spine lengths are useful morphometric characters for the species-level taxonomy of *Phrynus*. These new characters are used, together with traditional characters, to describe *Phrynus guarionexi* sp. nov. from the Dominican Republic. New data and comparative illustrations are also provided for *P. longipes*, the only other species of group B known to occur on Hispaniola, where it is widely distributed and sympatric with *P. guarionexi* sp. nov. (Figs. 1 and 2). Finally, new morphological data are provided concerning, among others, the cerotegument, frontal process and prolateral surface of the pedipalp tibia in the species of group B, along with a revised diagnosis of the group.

Together with Cuba, Hispaniola is one of the biodiversity hotspots of the Caribbean. With the description of *P. guarionexi* sp. nov., eleven whip spider species are now recorded in the Dominican Republic, eight phrynids (Quintero 1981; Armas 2006) and three charinids (Seiter et al., 2018). All species of *Charinus* Simon, 1892, i.e., *Charinus bahoruco* Teruel, 2016, *Charinus dominicanus* Armas and Calvo, 2001, and *Charinus magua* Seiter et al., 2018, and two species of *Phrynus*, i.e., *Phrynus kennidae* Armas and Calvo, 2001 and *P. guarionexi* sp. nov., recorded on Hispaniola appear to be range restricted (Armas 2006; Teruel 2016; Seiter et al., 2018).

2. Material and methods

2.1. Comparative material examined

The study sample comprised all species of *Phrynus* in group B except *P. panche*. Material is deposited in the collection of the Natural History Museum, Vienna, Austria (NHMW), the Natural History Museum, London, UK (BMNH), and the American Museum of Natural History, New York, U.S.A. (AMNH).

Phrynus araya Colmenares García and Villarreal, 2008: **Venezuela**: *Zulia State*: Sierra de Perijá, Municipio Machiques, Quebrada Kujane, before Ayajpaina, 1150 m, P.A. Colmenares, iv.2006, 2 \$\paralle{2}\$ (AMNH).

Phrynus calypso Chirivi-Joya, 2017: **Trinidad & Tobago:** Diego Martin Region: Trinidad, beside Tucker Valley Road, near Mount Pleasant, $10^{\circ}42'47.74''N$ $61^{\circ}36'36.39''W$, H.-W. Auer, iii.2014, $1 \stackrel{?}{\circ} (NHMW \ 27626)$, $3 \stackrel{?}{\circ} \stackrel{?}{\circ} (NHMW \ 27627)$, $1 \stackrel{?}{\circ}$, $1 \stackrel{?}{\circ} (NHMW \ 27628)$; Trinidad, Simla, Arima Valey, J.G. Rozen, Jr., 08.ii.1965, $6 \stackrel{?}{\circ} (AMN-H_IZC \ 00146677)$.

Phrynus exsul Harvey, 2003: **Indonesia:** East Nusa Tenggara Province: Gua Cermin, near Labuan Bajo, Flores, 08°28′33″S 119°53′46″E and Batu Cave Niki, near Warsawe, Flores, 08°32′S 119°59′E, M. Seiter, 2013—2015, captive bred, 2 ♂♂, 5 ♀♀ (NHMW 29684), 1 ♀ (NHMW 29851).

Phrynus goesii Thorell, 1889: **Lesser Antilles:** St. Maartin, D. Corrie, x.2010, $4 \, \text{dd}$, $2 \, \text{9P}$ (NHMW 28527), M. Seiter, xi.2011, $2 \, \text{dd}$, $1 \, \text{P}$ (NHMW 28528), iii.2017, $1 \, \text{dd}$, $2 \, \text{P}$ (NHMW 29705), 2019, $5 \, \text{dd}$, $11 \, \text{PP}$ (NHMW 29852).

Phrynus longipes (Pocock, 1894): **Dominican Republic:** La Altagracia Province: Boca de Yuma, Parque Nacional del Este, 18°22.528′N 68°36.914′W, M. Seiter, F. Schramm, J. Nigl and R. Teruel, ix.2016, 2 &\$\delta\$, 1 \(\frac{9}{2}\) (NHMW 29664), 1 \(\delta\$, 1 \(\frac{9}{2}\) (AMNH); same data except 18°21.403′N 68°37.450′W, 1 \(\delta\$ (AMNH). Monseñor Nouel Province: Subida a Casabíto, 19°01.643′N 70°22.762′W, 382 m, M. Seiter, F. Schramm, J. Nigl and R. Teruel, ix.2016, 1 \(\delta\$ (NHMW 29651), 2 \(\frac{9}{2}\) (NHMW 29652). Samaná Province: Cueva de Lolo, Casas del



Fig. 1. Whip spiders, *Phrynus guarionexi* sp. nov. (A—C) and *Phrynus longipes* (Pocock, 1894) (D—F), habitus in life. A. Paratype &, B. Paratype &, C. Juvenile, D. &, Samaná, Dominican Republic (D.R.). E. &, La Altagracia, D.R. F. &, Monseñor Nouel, D.R.

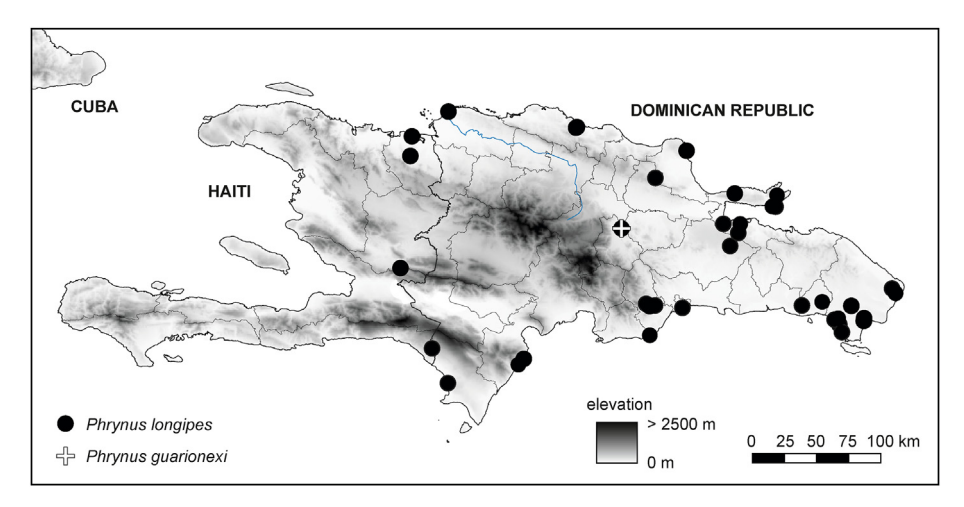


Fig. 2. Map of Hispaniola, plotting known localities of the whip spiders, Phrynus guarionexi sp. nov. and Phrynus longipes (Pocock, 1894), on the island.

Jamito, Las Terrenas, 19°16.917′N 69°33.380′W, 271 m, M. Seiter, F. Schramm, J. Nigl and R. Teruel, ix.2016, 5 ♂♂, 7 ♀♀ (NHMW 29660).

Phrynus pinarensis Franganillo, 1930: **Cuba: Pinar del Río Province: Cueva del Cable, Mogotela Guasasa, 22°33.668′N

83°49.982′W, 130 m, M. Seiter, F. Schramm, J. Nigl and R. Teruel, viii.2013, 1 $\stackrel{.}{\circ}$, 1 $\stackrel{.}{\circ}$ (NHMW 27634), 1 $\stackrel{.}{\circ}$, 5 $\stackrel{.}{\circ}$ (NHMW 29853); near Viñales, 22°40′01.7″N 83°42′27.9″W, 154 m, M. Seiter, F. Schramm, J. Nigl and R. Teruel, viii.2013, 1 $\stackrel{.}{\circ}$, 1 juv. (NHMW 29685).

Phrynus pulchripes (Pocock, 1894): **Venezuela:** *Nueva Esparta*: 2 ♂♂ (NHMW 27632), west of Cerro el Copey, Fuentidueno, 11°00.703′N 63°55.218′W, S. Huber.

Phrynus tessellatus (Pocock, 1894): K.H. Hyll, 1971, 1 $\stackrel{}{\circ}$, 1 $\stackrel{}{\circ}$ (BMNH). **St. Lucia:** 1 $\stackrel{}{\circ}$ (NHMW 1449); Fond de Jacques, G.A. Ramage, 13.iv.1889, 2 $\stackrel{}{\circ}$ $\stackrel{}{\circ}$, 1 $\stackrel{}{\circ}$ (BMNH). **St. Vincent:** H.H. Smith 1 $\stackrel{}{\circ}$, 1 $\stackrel{}{\circ}$ (BMNH); Mount Gay Estate (Leeward), H.H. Smith, 2 $\stackrel{}{\circ}$ $\stackrel{}{\circ}$ (BMNH).

2.2. Microscopy and imaging

Specimens were examined and imaged with a Nikon SMZ-25 stereomicroscope (Tokyo, Japan) equipped with a Nikon DS-Ri1 camera. Measurements were recorded using NIS-Elements BR ver. 5.02.00 (Nikon Instruments Inc., New York, U.S.A.). Digital images were processed using Adobe Photoshop® ver. 8.0 to optimize the contrast and brightness.

For scanning electron microscopy (SEM), half the dry carapace cuticle (exuvia) of each species was excised and mounted on a standard aluminum stub with conductive carbon tape. Samples were sputter coated with gold using a Leica EM SCD050 (Wetzlar, Germany). Coated samples were analyzed with a Zeiss Supra 55 VP scanning electron microscope (Jena, Germany).

2.3. Morphological nomenclature

Morphological nomenclature and measurements generally follow Quintero (1981); terminology of pedipalp and leg segments follows Harvey & West (1998); pedipalps are subdivided into: coxa, trochanter, femur, patella, tibia, tarsus and claw. Pedipalp dorsal spines are indicated by Arabic numerals and ventral spines by Roman numerals, following Weygoldt (2000). Different authors have offered different interpretations of the pedipalp tibial and tarsal spination; the nomenclature of Seiter & Lanner (2017) and Seiter & Wolff (2017) is followed in the present contribution. The nomenclature of trichobothria on the distitibia of leg IV follows Weygoldt (2000), terminology of the reproductive organs follows Giupponi & Kury (2013), and the description of the cerotegument ultrastructure follows Wolff et al. (2016, 2017) and Seiter et al. (2022).

The following abbreviations are used. Chelicerae: 1—3 prolateral row of teeth; a—c retrolateral row of teeth. Pedipalps: co-ls, tarsus, row of long setae; co-ss, tarsus, row of short setae; lsmd-s, tibia, large submedial dorsal spine; lsmv-s, tibia, large submedial ventral spine; rs, tibia, row of setae proximal to cleaning organ; sp1, sp3, tibia, dorsal spines 1 and 3; spl, spIII, tibia, ventral spines I and II. Leg IV trichobothria: basitibia: bt, basitibial; distitibia: bc, basocaudal; bf, basofrontal; sbf, sub-basofrontal; sc-x, x series caudal; sf-x, series frontal; stc, x series subterminal caudal; stf, x series subterminal frontal; tc, terminal caudal; tf, terminal frontal; tm, terminal medial. Reproductive organs: cs, claw-like sclerites; Fi, fistula; GO, gonopod, genital operculum; LaM, male genitalia, lamina medialis; LoD, male genitalia, lobus dorsalis; LoL1, male genitalia, lobus lateralis primus; LoL2, male genitalia, lobus lateralis secundus; PI, gonopod, processus internus.

2.4. Landmark-based geometric morphometrics and linear distance measurements

Two-dimensional landmark-based geometric morphometrics were used to analyze variation in the shape of the pedipalp patella. Due to the limited number of specimens available, the following three species were excluded from the analysis, i.e., *P. araya*, *P. panche*, and *P. pulchripes*. Geometric morphometric data were recorded from 95 individuals of seven species of *Phrynus* group B: *P. calypso* ($n_{\delta} = 5$; $n_{\varrho} = 8$); *P. exsul* ($n_{\delta} = 2$; $n_{\varrho} = 6$); *P. goesii* ($n_{\delta} = 12$; $n_{\varrho} = 16$); *P. guarionexi* sp. nov. ($n_{\delta} = 4$; $n_{\varrho} = 3$); *P. longipes* ($n_{\delta} = 10$;

 $n_{\circ}=11$); *P. pinarensis* ($n_{\circ}=2$; $n_{\circ}=8$); *P. tessellatus* ($n_{\circ}=4$; $n_{\circ}=4$). Specimens were positioned to allow imaging of the retrolateral surface of the pedipalp patella (see Fig. 3A). The resulting images were used to place landmarks using tpsDig2 ver. 2.31 (Rohlf 2015). When the sinistral pedipalp was imaged, the resulting images were flipped horizontally and vertically prior to landmark placement. All specimens of P. calypso, P. exsul, P. goesii, P. guarionexi sp. nov. and P. longipes were imaged in duplicate. Landmarks (LM) were placed by starting at the apex of major patella spine P1 (LM1) and moving distally, assigning landmarks at intersections between the retrodorsal margin of the patella and major patella spines P2, P3, P4, P5, and P6 as well as at the apices of the spines (LM2-17) (Fig. 3A). Smaller spines, sometimes observed between major spines, especially in larger specimens, were ignored. Patella spines P7 and P8, variable intraspecifically and often deformed or broken, were ignored. Instead, the next landmark was placed on the dorsalmost point of the junction between the patella and tibia (LM18). Except for junctions between the pedipalp segments, the retroventral margin of the patella lacks conspicuous features suitable for landmarking. To record its shape, a background curve was drawn along the margin, beginning at the ventralmost point of the junction between the patella and tibia (LM19) and ending at the ventralmost point of the junction between the patella and femur (LM28). The curve was resampled by length to extract ten landmarks and semilandmarks (LM19, SLM20-27, LM28). Finally, a background curve was drawn along the retrodorsal margin of the patella, beginning at the dorsalmost point of the junction between the patella and femur (LM29) and ending at the intersection between P1 and the retrodorsal margin (LM34). The curve was resampled by length to extract six landmarks and semi-landmarks (LM29, SLM30-33, LM34). After digitizing the landmarks and generating a .tps file, curve points were appended to landmarks with tpsUtil ver. 1.78 (Rohlf 2015), generating a total of 34 landmarks. The .tps file was submitted to the geometric morphometrics package geomorph ver. 3.3.2 (Adams et al., 2021; Baken et al., 2021) in R ver. 4.1.2 (R Core Team 2021) for the analysis. Shape variables were obtained from landmark data by generalized Procrustes analysis using the gpagen function. Mean shapes were subsequently generated for aligned replicates of specimens. A principal component analysis (PCA) of the Procrustes shape coordinates was performed using the gm.prcomp function. Images used for landmark placement, the resulting .tps file, and the R script used for the analysis are deposited in the Dryad Digital Repository (https://doi.org/10.5061/ dryad.k0p2ngf9z).

Linear distance measurements were also recorded to determine the length and width of the patella, as well as the length of patella spines P2, P3, P4, P5 and P6 (Figs. 4A and 5A). The length of the patella was defined as the distance between the dorsalmost point of the junction between the patella and tibia (LM18) and the midpoint between the dorsalmost and ventralmost points of the junction between the patella and femur (LM28 and LM29) (Fig. 3A). Patella width was measured perpendicular to the line describing patella length, starting at the midpoint of the base of spine P3 and ending at the retroventral margin of the patella (Fig. 4 and 5). Spine length was measured as the distance between the apex of the spine and the midpoint between the proximal and distal intersections of the spine with the retrodorsal margin of the patella (referred to hereafter as the "spine base midpoint") (Fig. 5A). Linear measurements were recorded from 101 individuals of nine species of Phrynus group B: *P. araya* ($n_{\vartheta} = 2$); *P. calypso* ($n_{\vartheta} = 5$; $n_{\vartheta} = 8$); *P. exsul* ($n_{\vartheta} = 2$; $n_{\circ}=6$); *P. goesii* ($n_{\circ}=12$; $n_{\circ}=16$); *P. guarionexi* sp. nov. ($n_{\circ}=4$; $n_{\S}=3$); *P. longipes* ($n_{\delta}=10$; $n_{\S}=11$); *P. pinarensis* ($n_{\delta}=2$; $n_{\S}=8$); *P. pulchripes* $(n_{\delta} = 2)$; *P. tessellatus* $(n_{\delta} = 6; n_{\varphi} = 4)$. Additionally, measurements available in the literature for the carapace, pedipalp patella length and leg I femur length were included, i.e., P. calypso

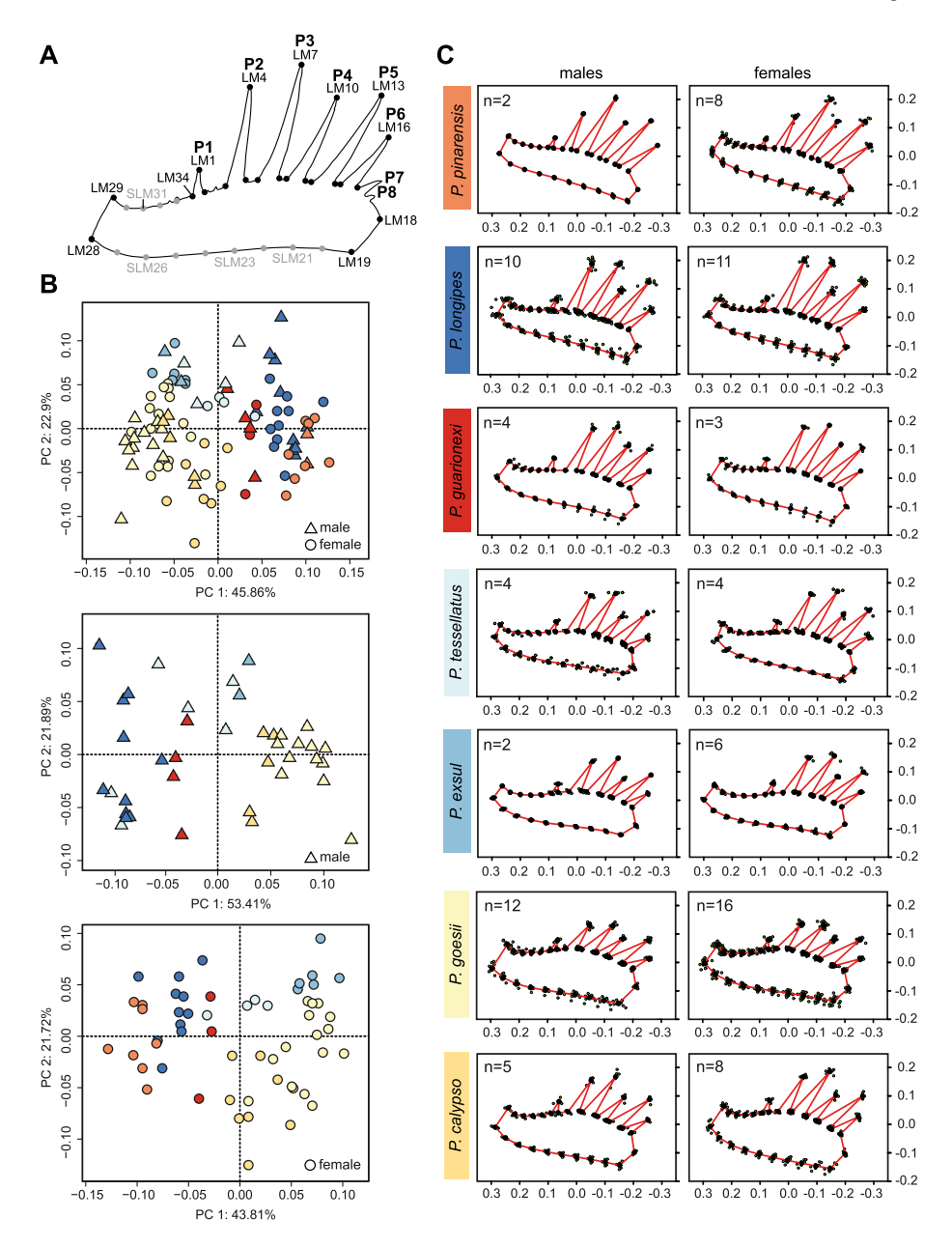


Fig. 3. Morphometrics and shape analysis in seven species of whip spiders of *Phrynus* Lamarck, 1801 group B. A. Landmarks used to analyze shape variation on retrolateral surface of pedipalp patella. B. Principal component analysis of Procrustes-aligned pedipalp patella landmarks, plotting first (PC1) and second (PC2) principal components for both sexes, respectively. Percentages in axis labels indicate proportion of variance explained by respective principal component. C. Plotted mean shape of Procrustes-aligned pedipalp patella for males and females, illustrating differences in shape. Black dots represent mean; green dots represent single specimen data; red line indicates average shape. Species color-coded in B and C. Abbreviations: LM, landmark; SML, semi-landmark; P1—P8, pedipalp patella dorsal spines 1—8. (For interpretation of references to color in this figure, see Web version.)

 $(n_{\delta}=5; n_{\varphi}=6)$ and *P. pulchripes* $(n_{\delta}=3; n_{\varphi}=3)$ (Chirivi-Joya 2017); *P. araya* $(n_{\delta}=1; n_{\varphi}=1)$ (Colmenares García and Villarreal, 2008). Leg I femur length measurements could not be obtained for the following specimens: *P. araya* $(n_{\varphi}=2)$; *P. calypso* $(n_{\delta}=3)$; *P. essul* $(n_{\varphi}=1)$; *P. goesii* $(n_{\delta}=5; n_{\varphi}=11)$; *P. guarionexi* sp. nov. $(n_{\delta}=1)$; *P. longipes* $(n_{\delta}=2)$; *P. tessellatus* $(n_{\delta}=6; n_{\varphi}=3)$. Carapace measurements could not be obtained for one male of *P. tessellatus* (compare Table S1).

2.5. Statistical tests

The distribution of ratios obtained from linear distance measurements per sex and species were each tested for normality with

a Shapiro-Wilk test using the package *stats* ver. 4.1.2 in R. As the hypothesis of normality was rejected for some distributions, nonparametric tests were performed to assess whether ratio distributions differed. A rank-based test for general factorial designs was performed in R, initially testing whether species and sex affect the distribution of a given linear distance measurement ratio and whether the effect of one factor (i.e., species or sex) on the given linear distance measure ratio depends on the level of the other factor (i.e., sex or species). The R package *rankFD* ver. 0.1.0 (Konietschke et al., 2021) was used for this procedure, by inputting the linear distance measurement ratios as response variables, and species and sex, as well as their interaction, as factor variables (ratio ~ species * sex). A Kruskal-Wallis rank sum test was

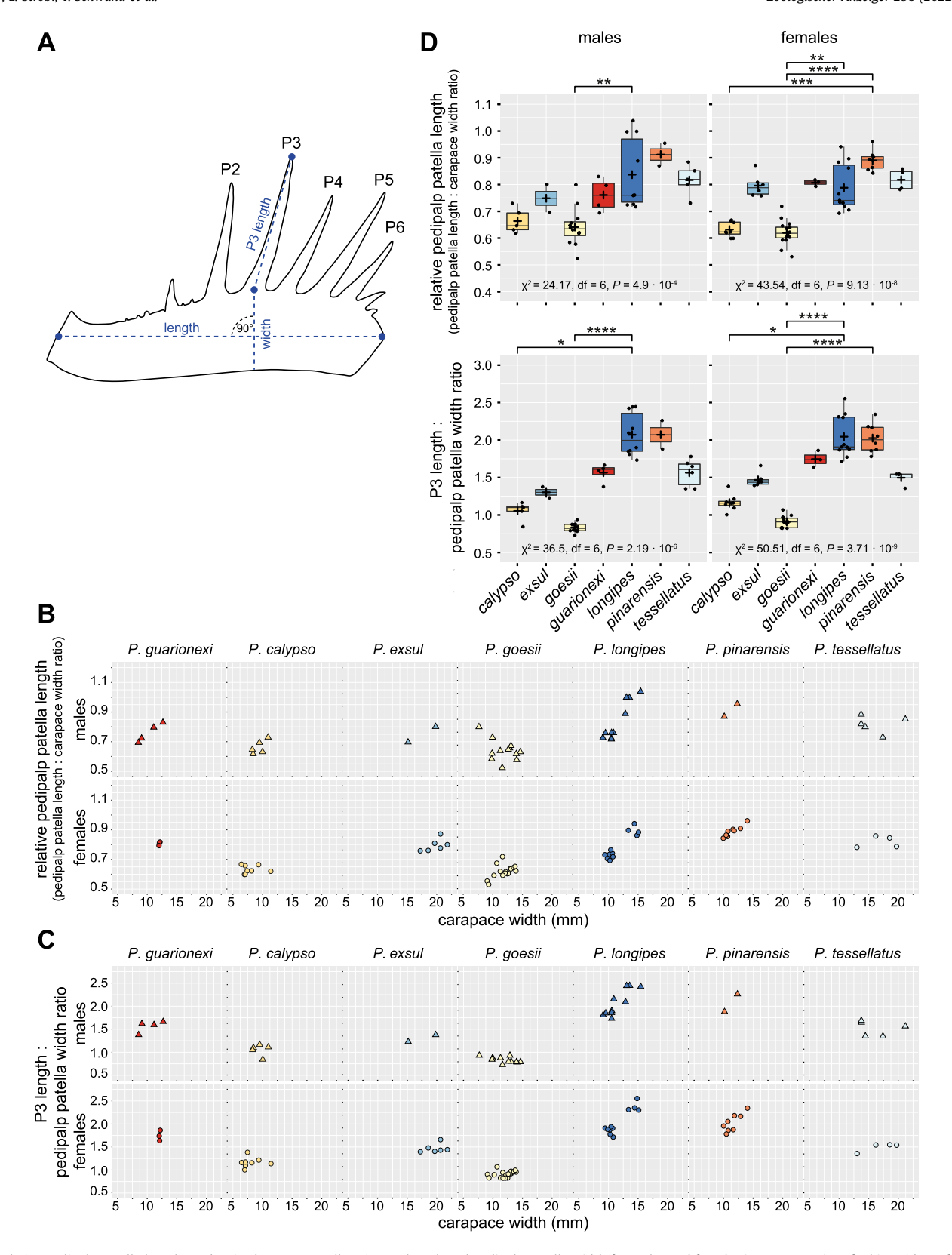


Fig. 4. Relative pedipalp patella lengths and ratios between patella spine P3 length and pedipalp patella width for males and females in seven species of whip spiders of *Phrynus* Lamarck, 1801 group B. **A.** Measurements of retrolateral surface and dorsal spines of pedipalp patella. **B.** Scatter plots showing relative pedipalp patella length plotted against carapace width. **C.** Scatter plots showing ratios between spine P3 length and pedipalp patella width plotted against carapace width. **D.** Boxplots of relative pedipalp patella length and spine P3 length: pedipalp patella width ratio. Crosses inside boxplots represent mean distributions. Kruskal-Wallis rank sum test results presented below boxplots. Bars above boxplots represent ratio distributions found to be significantly different following Dunn's test (all pairwise comparisons performed). *P* values Bonferroni-corrected according to number of comparisons (*, $P \le 0.05$; ***, $P \le 0.01$; ****, $P \le 0.001$; ****, $P \le 0.0001$). Specimen numbers: *P. calypso* ($n_{\sigma} = 5$; $n_{\varphi} = 8$); *P. essul* ($n_{\sigma} = 2$; $n_{\varphi} = 6$); *P. goesii* ($n_{\sigma} = 12$; $n_{\varphi} = 16$); *P. guarionexi* sp. nov. ($n_{\sigma} = 4$; $n_{\varphi} = 3$); *P. longipes* ($n_{\sigma} = 10$; $n_{\varphi} = 11$); *P. pinarensis* ($n_{\sigma} = 2$; $n_{\varphi} = 8$). *P. tessellatus* ($n_{\sigma} = 5$ in scatter plots and relative pedipalp patella length boxplot/6 in spine P3 length: pedipalp patella width ratio boxplot; $n_{\varphi} = 4$).

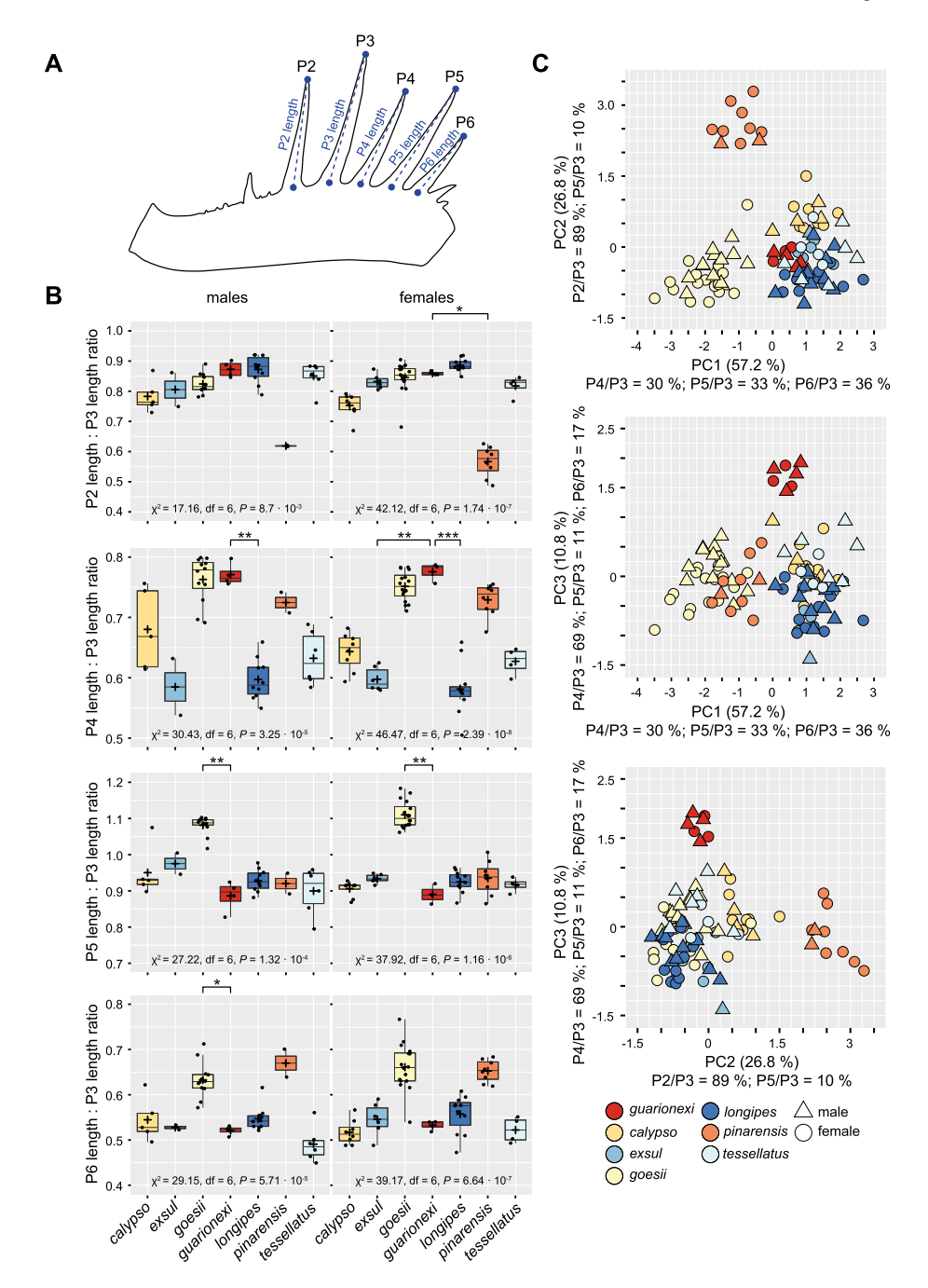


Fig. 5. Ratios between pedipalp patella dorsal spine lengths in seven species of whip spiders of *Phrynus* Lamarck, 1801 group B. **A.** Boxplots of ratios between pedipalp patella dorsal spine lengths. Crosses inside boxplots represent mean distributions. Kruskal-Wallis rank sum test results presented below boxplots. Bars above boxplots represent ratio distributions found to be significantly different following Dunn's test (pairwise comparisons between *P. guarionexi* sp. nov. and other species). *P* values Bonferroni-corrected according to number of comparisons (*, $P \le 0.05$; **, $P \le 0.01$; ****, $P \le 0.001$; ****, $P \le 0.001$). **C.** Principal component analysis of pedipalp patella dorsal spine length ratios. Plots show either first (PC1) and second (PC2), first (PC1) and third (PC3), or second (PC2) and third (PC3) principal components, respectively. Percentages representing proportion of variance explained by respective principal component in brackets and variables with contribution to principal component $\ge 10\%$ indicated together with percentage contribution. Specimen numbers: *P. calypso* ($n_{\sigma} = 5$; $n_{2} = 8$); *P. exsul* ($n_{\sigma} = 2$; $n_{2} = 6$); *P. goesii* ($n_{\sigma} = 12$; $n_{2} = 16$); *P. guarionexi* sp. nov. ($n_{\sigma} = 4$; $n_{2} = 3$); *P. longipes* ($n_{\sigma} = 10$; $n_{2} = 11$); *P. pinarensis* ($n_{\sigma} = 2$; $n_{2} = 8$); *P. tessellatus* ($n_{\sigma} = 6$; $n_{2} = 4$).

subsequently conducted on the linear distance measurement ratio datasets separated by sex using the R package *stats*, to test whether, for males and females respectively, species affect the distribution of a given linear distance measurement ratio. After the Kruskal-Wallis tests were statistically significant, a Dunn's multiple comparison test was performed as a post-hoc test, using the R package *rstatix* ver. 0.7.0 (Kassambara 2021), to test whether distance

measurement ratios differed from one another in pairwise comparisons. Dunn's test P values were Bonferroni-corrected by multiplication with the number of comparisons. A significance level of 5% was used as a threshold in the initial rankFD test, hence the adjusted P values obtained from the Dunn's test for male and female distribution comparisons were adjusted by multiplying by two.

3. Results

3.1. Pedipalp patella geometric morphometrics

The dataset presented herein exhibits overlapping specimen size ranges for P. calypso, P. goesii, P. guarionexi sp. nov., P. longipes and *P. pinarensis* (carapace widths ranging from ca. 6.5–15.5 mm). Specimens of *P. exsul* and *P. tessellatus* were larger (carapace widths ranging from ca. 13–21.7 mm) (Fig. 4B, C, S2–3). Plotting the first (PC1) and second (PC2) principal components (46% and 23% of the variance, respectively) obtained from a PCA of the Procrustesaligned pedipalp patella landmarks of male and female specimens revealed that specimens clustered largely according to the nominal species with overlap between adjacent species clusters (Fig. 3B). A clustering in accordance with the nominal species was also observed when PC1 and PC2 were plotted from PCAs based on males or females only (PC1, 53%, and PC2, 22%, in males; PC1, 44%, and PC2, 22%, in females) (Fig. 3B). Pronounced differences in shape were observed when the mean shape of the Procrustes-aligned patella was plotted for each species, whereas pedipalps of conspecific males and females appeared generally more similar to one another than to other species (Fig. 3C). Differences among the species were particularly obvious in the relationship between patella width and spine lengths as well as the relationship among spine lengths. Phrynus longipes and P. pinarensis possessed the slenderest pedipalp patella with the longest spines, whereas P. calypso and P. goesii possessed the broadest pedipalp patella with comparatively short spines, in *P. goesii*. These species are situated at opposite ends of the axis formed by PC1 whereas the other species. in which the pedipalp patella is more intermediate in shape, are located in between (Fig. 3B).

3.2. Pedipalp patella linear measurements

Linear measurements of patella lengths and widths and dorsal spine lengths were recorded to determine the insights revealed by the landmark-based morphometry on characters suitable for species diagnosis and to validate previously reported spine formulas in the species of Phrynus group B (Tables 1, 2, 4, S1; Figs. 4 and 5, S1-3). Plotting the relative pedipalp patella length (pedipalp patella length: carapace width ratio) against the carapace width suggests that, in P. longipes and P. pinarensis, the increase in pedipalp length shows positive allometry for both males and females (Fig. 4B). Further, the sample of *P. longipes* indicates that, at larger body sizes (ca. 15 mm carapace width), males present relatively longer pedipalp patellae than females. A relationship between relative pedipalp patella length and specimen carapace width is less obvious in the datasets of other species, as are possible differences among the sexes (Fig. 4B). Generally similar trends were indicated when the patella spine P3 length: pedipalp patella width ratio (Fig. 4C) and the relative leg I femur length (leg I femur length : carapace width ratio; Fig. S1A) were plotted against carapace width, again suggesting that ratios change allometrically in P. longipes and P. pinarensis.

Comparison of the distributions of relative pedipalp patella lengths, the spine P3 length: pedipalp patella width ratio, and the relative leg I femur length indicates similar differences among species for all three morphometric values (Figs. 4D and S1B). Nonparametric tests for the two-way factorial design (factors: sex and species, and their interaction; test performed using rankFD) suggest that, for the three morphometric values, significant differences exist among species whereas there is no evidence that ratios differ among conspecific males and females (Table 3). Sex alone was not found to influence the distribution of relative pedipalp patella lengths and relative leg I femur lengths, but

significantly influenced the distributions of the ratios between spine P3 length and pedipalp patella width. Accordingly, relative differences in the distributions of the three morphometric values among species appear similar when comparing males and females (Figs. 4D and S1B). Kruskal-Wallis tests comparing ratio distributions between species separated by sex suggest that, for the three morphometric values, distributions are significantly different among species (Figs. 4D and S1B). *Phrynus longipes* and *P. pinarensis* exhibit the relatively longest pedipalp patellae, the longest P3 spines in relation to pedipalp width, and the relatively longest leg I femurs, whereas the opposite is true for *P. calypso* and *P. goesii*. Intermediate phenotypes are evident in *P. exsul*, *P. guarionexi* sp. nov., and *P. tessellatus*. Pairwise comparison of ratio distributions among all species with a Dunn's test indicated statistically significant differences between several species (labeled in Figs. 4D and S1B).

Compared to relative pedipalp patella length, the ratio between spine P3 length and patella width as well as relative leg I femur length (Figs. 4B, C, S1A), the scatter plots of different patella dorsal spine length ratios plotted against carapace width did not suggest that spine length ratios change noticeably with size (Figs. S2 and 3). Nonparametric tests for the two-way factorial design (factors: sex and species, and their interaction; test performed using rankFD) suggest significant differences among species for all patella prodorsal spine ratios, whereas there is no evidence that ratios differ among conspecific males and females, or that sex influences the distribution thereof (Table 5). Relative differences among species are similar when comparing male and female spine ratio distributions (Fig. 5B). Kruskal-Wallis tests comparing pedipalp patella dorsal spine length ratio distributions between species separated by sex suggest that dorsal spine length ratio distributions are significantly different among species (Fig. 5B). The distribution of spine length ratios largely confirm qualitative spine formulas established in previously described species of Phrynus group B (Fig. 5B, Table 1): the spine formula of *P. calypso*, *P. exsul*, *P. longipes* and P. tessellatus is P3 > P5 > P2 > P4 > P6 > P1, and of P. pinarensis, P3 > P5 > P4 > P6 > P2 > P1. However, the spine formula of *P. goesii* derived from these data is P5 > P3 > P2 > P4 > P6 > P1, unlike the formula $P3 \ge P5 > P4 > P2 > P6 > P1$, suggested by Quintero (1981).

Phrynus guarionexi sp. nov. presents the same qualitative spine formula as the allopatric species *P. calypso*, *P. exsul* and *P. tessellatus* and the sympatric species *P. longipes*, i.e., P3 > P5 > P2 > P4 > P6 > P1. Thus, the ratios of P2: P3, P5: P3 and P6: P3 in *P. guarionexi* sp. nov. are similar to those of *P. calypso*, *P. exsul*, *P. longipes* and *P. tessellatus* but differ from those of *P. goesii* and *P. pinarensis*. *Phrynus guarionexi* sp. nov. bears a longer P2 spine in relation to P3 than in *P. pinarensis*, a shorter P5 spine in relation to P3 than in *P. goesii*, and a shorter P6 spine in relation to P3 when compared to both species. Post-hoc

Table 1Comparison of pedipalp patella spine formula (length of dorsal spines) among whip spiders of *Phrynus* Lamarck, 1801 group B (Quintero 1981). Data for *Phrynus araya* Colmenares García and Villarreal, 2008 and *Phrynus panche* Armas and Angarita, 2008 measured from original illustrations (Colmenares García and Villarreal, 2008; Armas and Angarita, 2008).

| | patella spine P1—P6 formula |
|----------------|-----------------------------|
| P. araya | P3 > P5 > P2 > P4 > P6 > P1 |
| P. calypso | P3 > P5 > P2 > P4 > P6 > P1 |
| P. exsul | P3 > P5 > P2 > P4 > P6 > P1 |
| P. goesii | P5 > P3 > P2 > P4 > P6 > P1 |
| P. guarionexi | P3 > P5 > P2 > P4 > P6 > P1 |
| P. longipes | P3 > P5 > P2 > P4 > P6 > P1 |
| P. panche | P3 > P5 > P2 > P4 > P6 > P1 |
| P. pinarensis | P3 > P5 > P4 > P6 > P2 > P1 |
| P. pulchripes | P3 > P5 > P2 > P4 > P6 > P1 |
| P. tessellatus | P3 > P5 > P2 > P4 > P6 > P1 |
| | |

Table 2

Comparison of ratio between pedipalp patella length and carapace width, ratio between patella spine P3 length and pedipalp patella width, and ratio between leg I femur length and carapace width among whip spiders of *Phrynus* Lamarck, 1801 group B (Quintero 1981); mean ± SD, data in square brackets represent minimum and maximum values. Data for *Phrynus panche* Armas and Angarita, 2008 measured from original illustrations (Armas and Angarita, 2008); data for *Phrynus araya* Colmenares García and Villarreal, 2008, *Phrynus calypso* Chirivi-Joya, 2017 and *Phrynus pulchripes* (Pocock, 1894) combined from literature data and present study (compare Table S1). Data from Armas and Angarita (2008)¹, Colmenares García and Villarreal (2008)², and Quintero (1981)³. *Phrynus tessellatus* (Pocock, 1894) illustrated by Seiter & Lanner (2017) = *Phrynus calypso* (Chirivi-Joya 2017). HT = holotype; PT = paratype.

| | pedipalp patella length : carapace width ratio | patella spine P3 length : pedipalp patella width ratio | leg I femur length : carapace width ratio |
|----------------|--|--|--|
| P. araya | HT\$ 0.74 n = 1 ² | HT \circ 2.12 $n = 1^2$ | HT♀ 1.93 n = 1 ² |
| - | PT1♀ 0.64 n = 1 | PT19 0.84 n = 1 | |
| | PT2♀ 0.68 n = 1 | PT2♀ 1.35 n = 1 | |
| P. calypso | $30.66 \pm 0.05 [0.62 - 0.73] n = 8$ | ♂ 1.05 ± 0.12 [0.84–1.17] n = 5 | $\stackrel{\circ}{}$ 1.77 ± 0.16 [1.55−2.08] $n = 8$ |
| | $90.62 \pm 0.05 [0.49 - 0.67] n = 13$ | $91.17 \pm 0.11 [1-1.38] n = 8$ | $91.65 \pm 0.19 [1.30 - 1.88] n = 13$ |
| P. exsul | ♂ 0.75 ± 0.07 [0.7–0.8] n = 2 | ♂ 1.3 ± 0.1 [1.23–1.38] n = 2 | δ 1.82 ± 0.01 [1.75−1.89] $n = 2$ |
| | $9.08 \pm 0.04 [0.76 - 0.87] n = 6$ | $91.47 \pm 0.1 [1.4 - 1.66] n = 6$ | $91.84 \pm 0.09 [1.73 - 1.94] n = 5$ |
| P. goesii | ♂ 0.64 ± 0.07 [0.52–0.8] n = 12 | ♂ 0.84 ± 0.06 [0.73-0.93] n = 12 | $\delta 1.42 \pm 0.11 [1.3 - 1.62] n = 7$ |
| | $9.62 \pm 0.04 [0.53 - 0.72] n = 16$ | $90.91 \pm 0.07 [0.82 - 1.07] n = 16$ | $91.38 \pm 0.16 [1.17 - 1.57] n = 5$ |
| P. guarionexi | $3.076 \pm 0.06 [0.69 - 0.83] n = 4$ | ♂ 1.57 ± 0.13 [1.38–1.67] n = 4 | $3.2.05 \pm 0.06 [1.98 - 2.11] n = 3$ |
| | $9.81 \pm 0.01 [0.79 - 0.82] n = 3$ | $91.75 \pm 0.11 [1.64 - 1.86] n = 3$ | $92.1 \pm 0.15 [1.93 - 2.21] n = 3$ |
| P. longipes | $30.84 \pm 0.13 [0.72 - 1.04] n = 10$ | ♂ 2.07 ± 0.28 [1.73–2.45] n = 10 | $3.76 \pm 0.23 [2.4 - 3.13] n = 8$ |
| | $90.79 \pm 0.09 [0.69 - 0.94] n = 11$ | $2.05 \pm 0.28 [1.72 - 2.55] n = 11$ | $92.47 \pm 0.31 [2.13 - 3.01] n = 11$ |
| P. panche | HT σ 0.73 $n = 1^{1}$ | $HT \stackrel{\circ}{\circ} 1.16 n = 1^{1}$ | $HT \stackrel{\circ}{\circ} 1.24 \ n = 1^1$ |
| P. pinarensis | ♂ 0.91 ± 0.06 [0.87–0.95] n = 2 | ♂ 2.07 ± 0.27 [1.88-2.26] n = 2 | $32.73 \pm 0.01 [2.73 - 2.74] n = 2$ |
| | $9.089 \pm 0.04 [0.84 - 0.96] n = 8$ | $2.03 \pm 0.19 [1.78 - 2.34] n = 8$ | $92.57 \pm 0.11 [2.43 - 2.74] n = 8$ |
| P. pulchripes | $30.73 \pm 0.06 [0.64 - 0.79] n = 5$ | ♂ 0.97 ± 0.2 [0.77-1.18] n = 2 | $\delta 1.63 \pm 0.15 [1.39 - 1.80] n = 5$ |
| | $9.067 \pm 0.04 [0.64 - 0.71] n = 3$ | | $91.52 \pm 0.10 [1.46 - 1.64] n = 3$ |
| P. tessellatus | ♂ 0.82 ± 0.06 [0.73–0.88] n = 5 | ♂ 1.56 ± 0.18 [1.35–1.78] n = 6 | ♀ 1.6 <i>n</i> = 1 |
| | $9.0.82 \pm 0.04 [0.78 - 0.86] n = 4$ | $91.5 \pm 0.09 [1.36 - 1.55] n = 4$ | $HT \delta 1.66 n = 1^3$ |

Table 3RankFD test results (ANOVA-type statistic) for relative pedipalp patella length, ratio of patella spine P3 length: pedipalp patella width patella width and relative leg I femur length among whip spiders of *Phrynus* Lamarck, 1801 group B (Quintero 1981)

| Factor | Statistic | df1 | df2 | P | | | | |
|---|--|------|-------|----------|--|--|--|--|
| Relative pedipal | Relative pedipalp patella length (patella length : carapace width ratio) | | | | | | | |
| Species | 23.82 | 4.05 | 8.61 | 0.0001 | | | | |
| Sex | 0.0027 | 1 | 8.61 | 0.96 | | | | |
| Species:Sex | 0.77 | 4.05 | 8.61 | 0.57 | | | | |
| Patella spine P3 | Patella spine P3 length : pedipalp patella width ratio | | | | | | | |
| Species | 111.01 | 4.65 | 20.99 | < 0.0001 | | | | |
| Sex | 4.49 | 1 | 20.99 | 0.046 | | | | |
| Species:Sex | 1.95 | 4.65 | 20.99 | 0.13 | | | | |
| Relative leg I femur length (leg I femur length : carapace width ratio) | | | | | | | | |
| Species | 92.14 | 2.78 | 6.12 | < 0.0001 | | | | |
| Sex | 3.06 | 1 | 6.12 | 0.13 | | | | |
| Species:Sex | 1.08 | 2.78 | 6.12 | 0.42 | | | | |

Dunn's tests comparing ratio distributions in *P. guarionexi* sp. nov. to those of the other species indicated that most of the differences between *P. guarionexi* sp. nov., *P. goesii* and *P. pinarensis* are statistically significant (Fig. 5B). Although *P. guarionexi* sp. nov. shares the same spine formula as *P. calypso*, *P. exsul*, *P. longipes*, and *P. tessellatus*, the P4 spines of this species are longer in relation to P3: *P. calypso*, mean $\delta = 0.68 \pm 0.07$, $9 = 0.64 \pm 0.03$; *P. exsul*, mean 0.68 ± 0.07 , $9 = 0.64 \pm 0.03$; *P. exsul*, mean 0.68 ± 0.07 , 1.69 ± 0.07 , 1.69 ± 0.09 ; *P. longipes*, mean 1.69 ± 0.09 , 1.69 ± 0.09 ; *P. longipes*, mean 1.69 ± 0.09 , 1.69 ± 0.09 ; *P. tessellatus*, mean 1.69 ± 0.09 ; *P. longipes*, mean 1.69 ± 0.09 ; *P. tessellatus*, mean 1.69 ± 0.09 ; *P. guarionexi* sp. nov. to male and female *P. longipes* (comparison 1.69 ± 0.09), and when comparing female *P. guarionexi* sp. nov. to female *P. exsul* (1.69 ± 0.09).

A principal component analysis of the four spine ratios, with male and female specimens pooled, revealed the presence of three non-overlapping clusters, corresponding to the three qualitative spine formulas known for the species of *Phrynus* group B, when the first two principal components were plotted (Fig. 5C). *Phrynus guarionexi* sp. nov. specimens clustered together with *P. calypso*,

P. exsul, P. longipes and *P. tessellatus* to the exclusion of *P. goesii* and *P. pinarensis*. However, when the third principal component (PC3) was plotted against either the first (PC1) or second (PC2), respectively, the specimens of *P. guarionexi* sp. nov. clustered to the exclusion of all other species of *Phrynus* group B. The variable contributions of 69% for the P4: P3 ratio and 17% for the P6: P3 ratio towards PC3 suggest that *P. guarionexi* sp. nov. can be distinguished from all other species of *Phrynus* group B investigated, by these two ratios alone.

3.3. Cerotegument ultrastructure

The cerotegument of all specimens investigated forms globular structures with a diameter of 0.8-3.8 µm (Fig. 6). The diameters of the globules observed in P. guarionexi sp. nov. and a specimen of P. longipes from Samaná were 2.0-2.2 μm and 1.8-2.2 μm, respectively. The globules were larger (3.4–3.8 μm in diameter) in a specimen of *P. longipes* from La Altagracia but smaller (0.8–1.4 μm in diameter) in a specimen of P. longipes from Monseñor Nouel, the population sympatric with P. guarionexi sp. nov. The globule surface was highly corrugated in P. guarionexi sp. nov. (Fig. 6A and B) whereas the surfaces were wrinkled with dimples in P. longipes (Fig. 6C–H). The colloidal particles were lamelliform in *P. guarionexi* sp. nov. and crystalline or coralline in P. longipes. The colloidal particles of both species were small and interconnected but did not assemble completely on the globule surface. Almost the entire globule surface was covered with coralline colloidal particles in the specimens of P. longipes from La Altagracia (Fig. 6E and F) and Monseñor Nouel (Fig. 6G and H), whereas gaps were visible in the specimen from Samaná (Fig. 6C and D; Seiter et al., 2022).

3.4. Taxonomy

3.4.1. Phrynus Lamarck, 1801

Diagnosis: *Phrynus* may be separated from other genera of Phrynidae Blanchard, 1852, by the following combination of characters: carapace anterior margin with short spines (denticuliform tubercles) or almost smooth (cf. *Acanthophrynus coronatus*

Table 4
Comparison of pedipalp patella dorsal spine length ratios among whip spiders of *Phrynus* Lamarck, 1801 group B (Quintero 1981); mean ± SD, data in square brackets represent minimum and maximum values. Data for *Phrynus araya* Colmenares García and Villarreal, 2008 and *Phrynus panche* Armas and Angarita, 2008 measured from original illustrations (Colmenares García and Villarreal, 2008; Armas and Angarita, 2008) except for additional measurements for paratype (PT) specimens of *P. araya*. Data from Colmenares García and Villarreal (2008)¹; Armas and Angarita (2008)². HT = holotype; PT = paratype.

| | spine P2 length: P3 length ratio | spine P4 length: P3 length ratio | spine P5 length: P3 length ratio | spine P6 length: P3 length ratio |
|----------------|--|---|---|---|
| P. araya | HT♀ 0.85 n = 1 ¹ | HT♀ 0.75 n = 1 ¹ | HT♀ 0.85 n = 1 ¹ | HTP 0.50 n = 1 ¹ |
| | PT1 $0.71 \ n = 1$ | PT1 $0.76 \ n = 1$ | PT1 1.05 $n = 1$ | PT1 $0.64 n = 1$ |
| | PT2 $0.86 n = 1$ | PT2 $0.71 \ n = 1$ | PT2 0.88 $n = 1$ | PT2 $0.61 \ n = 1$ |
| P. calypso | $30.78 \pm 0.05 [0.73 - 0.87] n = 5$ | $\stackrel{?}{\circ}$ 0.68 ± 0.07 [0.61−0.76] $n = 5$ | $\stackrel{\circ}{}$ 0.95 ± 0.07 [0.9−1.08] $n = 5$ | $\stackrel{\circ}{\circ}$ 0.55 ± 0.05 [0.5−0.62] $n = 5$ |
| | $9.0.75 \pm 0.04 [0.67 - 0.79] n = 8$ | $9.0.64 \pm 0.03 [0.59 - 0.68] n = 8$ | $90.91 \pm 0.02 [0.87 - 0.93] n = 8$ | $9.0.52 \pm 0.03 [0.49 - 0.57] n = 8$ |
| P. exsul | $\stackrel{?}{\sim}$ 0.81 ± 0.08 [0.75−0.86] $n = 2$ | ਰੈ 0.59 ± 0.07 [$0.54-0.63$] $n=2$ | $\stackrel{?}{\circ}$ 0.98 ± 0.04 [0.95−1.01] $n = 2$ | δ 0.53 ± 0.01 [0.52−0.53] $n = 2$ |
| | $90.83 \pm 0.03 [0.81 - 0.87] n = 6$ | $9.06 \pm 0.02 [0.58 - 0.63] n = 6$ | $90.93 \pm 0.01 [0.92 - 0.95] n = 6$ | $9.0.55 \pm 0.04 [0.49 - 0.59] n = 6$ |
| P. goesii | $30.82 \pm 0.03 [0.78 - 0.89] n = 12$ | ♂ 0.76 ± 0.04 [0.69–0.8] n = 12 | δ 1.08 ± 0.03 [1.02−1.1] n = 12 | $\delta 0.63 \pm 0.04 [0.57 - 0.71] n = 12$ |
| | $90.85 \pm 0.05 [0.68 - 0.9] n = 16$ | $9.0.75 \pm 0.02 [0.71 - 0.78] n = 16$ | $91.11 \pm 0.04 [1.06 - 1.18] n = 16$ | $9.066 \pm 0.05 [0.54 - 0.77] n = 16$ |
| P. guarionexi | ♂ 0.87 ± 0.03 [0.85 – 0.9] $n = 4$ | ਰੈ 0.77 ± 0.02 $[0.76-0.8]$ $n=4$ | $\delta 0.89 \pm 0.04 [0.83 - 0.92] n = 4$ | $\stackrel{\circ}{\circ}$ 0.52 ± 0.01 [0.51−0.53] $n = 4$ |
| | $90.86 \pm 0.01 [0.86 - 0.87] n = 3$ | $9.0.78 \pm 0.02 [0.76 - 0.79] n = 3$ | $90.89 \pm 0.03 [0.86 - 0.92] n = 3$ | $90.53 \pm 0.01 [0.52 - 0.54] n = 3$ |
| P. longipes | $30.87 \pm 0.05 [0.79 - 0.92] n = 10$ | ਰੈ 0.60 ± 0.03 [$0.55-0.66$] $n = 10$ | δ 0.93 ± 0.03 [0.88−0.98] $n = 10$ | ♂ 0.55 ± 0.03 [0.52 – 0.62] $n = 10$ |
| | $90.89 \pm 0.02 [0.85 - 0.92] n = 11$ | $9.58 \pm 0.04 [0.51 - 0.66] n = 11$ | $90.93 \pm 0.03 [0.87 - 0.96] n = 11$ | $9.56 \pm 0.04 [0.47 - 0.61] n = 11$ |
| P. panche | HT $\vec{\sigma}$ 0.84 $n = 1^2$ | $HT \delta 0.73 \ n = 1^2$ | $HT 3 1.04 n = 1^2$ | $HT \circ 0.55 \ n = 1^2$ |
| P. pinarensis | $\stackrel{\circ}{\circ}$ 0.62 ± 0.003 [0.62−0.62] $n=2$ | $\stackrel{\circ}{\circ}$ 0.73 ± 0.02 [0.71−0.74] $n=2$ | δ 0.92 ± 0.04 [0.89−0.95] $n = 2$ | ਰੈ 0.67 ± 0.04 $[0.64-0.70]$ $n=2$ |
| | $9.0.57 \pm 0.05 [0.49 - 0.63] n = 8$ | $9.0.73 \pm 0.03 [0.68 - 0.76] n = 8$ | $90.94 \pm 0.05 [0.87 - 1.01] n = 8$ | $9.0.65 \pm 0.03 [0.62 - 0.68] n = 8$ |
| P. pulchripes | ♂ 0.85 ± 0.01 [0.85 - 0.86] $n = 2$ | ਰੈ 0.77 ± 0.01 [$0.76-0.78$] $n=2$ | δ 1.11 ± 0.09 [1.02−1.19] $n = 2$ | ♂ 0.67 ± 0.05 [0.62 – 0.72] $n = 2$ |
| P. tessellatus | ਰੈ 0.85 ± 0.05 $[0.76-0.88]$ $n = 6$ | $30.63 \pm 0.04 [0.58 - 0.69] n = 6$ | $\delta 0.90 \pm 0.07 [0.8 - 0.96] n = 6$ | ਰੈ $0.49 \pm 0.04 [0.45-0.56] n = 6$ |
| | $9.0.82 \pm 0.04 [0.77 - 0.85] n = 4$ | $90.63 \pm 0.02 [0.6-0.65] n = 4$ | $90.92 \pm 0.02 [0.9 - 0.94] n = 4$ | $9.0.52 \pm 0.03 [0.49 - 0.55] n = 4$ |

Table 5RankFD test results (ANOVA-type statistic) for pedipalp patella dorsal spine length ratios among whip spiders of *Phrynus* Lamarck, 1801 group B (Quintero 1981).

| Factor | Statistic | df1 | df2 P | | | | |
|---|-------------------|---------|-------|----------|--|--|--|
| patella spine P2 length : P3 length ratio | | | | | | | |
| Species | 14.6 | 2.56 | 3.28 | 0.022 | | | |
| Sex | 0.3 | 1 | 3.28 | 0.62 | | | |
| Species:Sex | 0.96 | 2.56 | 3.28 | 0.49 | | | |
| patella spine P4 | length : P3 lengt | h ratio | | | | | |
| Species | 33.64 | 3.22 | 4.62 | 0.0014 | | | |
| Sex | 0.43 | 1 | 4.62 | 0.544 | | | |
| Species:Sex | 0.32 | 3.22 | 4.62 | 0.8224 | | | |
| patella spine P5 | length : P3 lengt | h ratio | | | | | |
| Species | 9.04 | 3.15 | 5.5 | 0.014 | | | |
| Sex | 0.9 | 1 | 5.5 | 0.38 | | | |
| Species:Sex | 0.5 | 3.15 | 5.5 | 0.71 | | | |
| patella spine P6 length : P3 length ratio | | | | | | | |
| Species | 21.87 | 4.54 | 29.4 | < 0.0001 | | | |
| Sex | 1.05 | 1 | 29.4 | 0.31 | | | |
| Species:Sex | 1.04 | 4.54 | 29.4 | 0.41 | | | |

Kraepelin, 1899); prolateral row of cheliceral teeth with three cuspid denticles, the ventralmost tooth (distal: 3) bicuspid; retrodorsal margin of pedipalp patella with one spine (P4) between the two longest (P3 and P5) spines; tarsus of leg I without arolium, except in protonymphal stage; tibia of leg IV comprising three or four articles.

3.4.2. Key to identification of species in group B of Phrynus Lamarck, 1801

- 1. Chelicera retrolateral margin with one tooth ... *Phrynus pinarensis* Franganillo, 1930
 - Chelicera retrolateral margin with > one tooth ... 2
- 2. Chelicera retrolateral margin with three teeth ... 3
 - Chelicera retrolateral margin with two teeth ... 7
- 3. Leg IV distitibia with > 30 trichobothria ... *Phrynus longipes* (Pocock, 1894)
 - Leg IV distitibia with \leq 30 trichobothria ... 4.
- 4. Pedipalp patella dorsal spines relative length, P5 > P3 > P2 > P4 > P6 > P1 ... Phrynus goesii Thorell, 1889

- Pedipalp patella dorsal spines relative length, P3 > P5 > P2 > P4 > P6 > P1 ... 5
- 5. Female genital sclerite rectilinear, with apex uncurved, base much broader than apex; pedipalp patella spine P4 length: spine P3 length ratio, 0.76–0.8 (mean, 0.77) ... *Phrynus guarionexi* sp. nov.
 - Female genital sclerite acuminate, with apex curved; pedipalp patella spine P4 length: spine P3 length ratio, < 0.76 ... 6
- 6. Female genital sclerite with base much broader than apex; pedipalp patella spine P4 length: spine P3 length ratio, 0.59–0.76 (mean, 0.66); pedipalp patella spine P3 length: patella width ratio, 0.84–1.38 (mean, 1.12); leg IV distitibia with 23 trichobothria ... *Phrynus calypso* Chirivi-Joya, 2017
 - Female genital sclerite with base slightly broader than apex; pedipalp patella spine P4 length: spine P3 length ratio, 0.58–0.69 (mean, 0.63); pedipalp patella spine P3 length: patella width ratio, 1.35–1.78 (mean, 1.54); leg IV distitibia with 25 trichobothria ... *Phrynus tessellatus* (Pocock, 1894)
- 7. Leg I femur length: carapace width ratio < 1.3 ... *Phrynus panche* Armas and Angarita, 2008
 - Leg I femur length: carapace width ratio > 1.3 ... 8
- 8. Leg IV distitibia with > 30 trichobothria ... *Phrynus exsul* Harvey, 2003
 - Leg IV distitibia with < 30 trichobothria ... 9
- 9. Leg IV distitibia with 26 trichobothria; leg I femur length : carapace width ratio maximum, 1.93 (\$\partial \text{...} \text{ Phrynus araya Colmenares García and Villarreal, 2008}
 - Leg IV distitibia with 24 trichobothria; leg I femur length: carapace width ratio maximum, 1.64 (♀) or 1.80 (♂) ... Phrynus pulchripes (Pocock, 1894)

3.4.3. Phrynus guarionexi sp. nov.

Type Material: Dominican Republic: *Monseñor Nouel Province*: Subida a Casabíto, 19°01.643′N 70°22.762′W, 382 m, M. Seiter, F. Schramm, J. Nigl and R. Teruel, ix.2016; holotype ♀ (NHMW 29647), paratypes: 1 ♂ (NHMW 29648), 1 ad. [partly destroyed] (NHMW 29649), 1 ♂, 1 ♀ with egg sac (NHMW 29650), 1 ♂, 1 ♀ (AMNH).

Etymology: The species is named after Guarionex, the historical Taíno cacique (king, chief) of Maguá, a region that presently

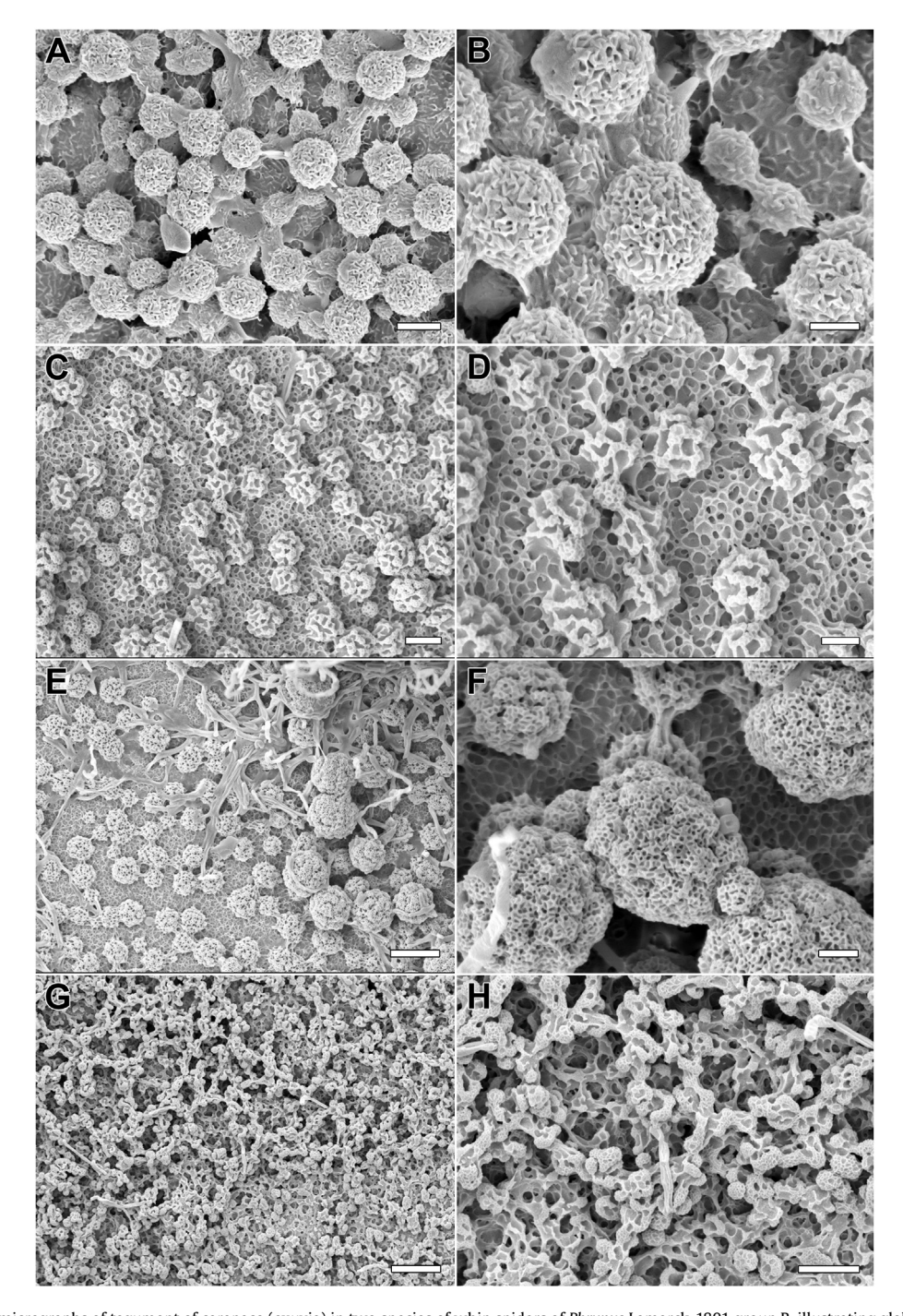


Fig. 6. Scanning electron micrographs of tegument of carapace (exuvia) in two species of whip spiders of *Phrynus* Lamarck, 1801 group B, illustrating globular structures (**A**, **C**, **E**, **G**) and colloidal particles (**B**, **D**, **F**, **H**). **A**, **B**. *Phrynus guarionexi* sp. nov., Monseñor Nouel, Dominican Republic (D.R.). **C**–**H**. *Phrynus longipes* (Pocock, 1894): **C**, **D**. Samaná, D.R.; **E**, **F**. La Altagracia, D.R.; **G**, **H**. Monseñor Nouel, D.R. Scale bars: 2 μm (**A**, **C**); 1 μm (**B**, **D**, **F**); 4 μm (**E**); 6 μm (**G**); 3 μm (**H**).

includes parts of Monseñor Nouel Province in the Dominican Republic.

Diagnosis: *Phrynus guarionexi* sp. nov. may be assigned unequivocally to group B based on the presence of an inconspicuous spine on the prodorsal surface of the pedipalp tarsus. Together with this character, it may be distinguished from all other *Phrynus* species by means of the following combination of characters: carapace frontal process present but weakly developed in male, weakly to strongly developed, pointed in female; male genitalia with PI small, blunt but prominent, LaM large, cuspid, LoD large, partly sclerotized with blunt but pointed apex; female gonopod evenly

sclerotized, with two claw-like appendages, intermediate length (compared to others), hard, cuspid, base much wider than apex, rectilinear with straight, rounded apex; retrolateral margin of chelicera with three teeth; prolateral surface of pedipalp tibia granular with many setiferous tubercles; pedipalp patella length: carapace width ratio, 0.69–0.83; proventral surface of pedipalp trochanter with three large spines; pedipalp patella spine P3 length: patella width ratio, 1.38–1.86; patella spine P2 length: spine P3 length ratio, 0.76–0.8; spine P5 length: spine P3 length ratio, 0.83–0.92; spine P6 length: spine P3 length ratio, 0.51–0.54; pedipalp tibia sp3

prominent, approximately two-thirds length of lsmd-s (sp2); pedipalp tibia spIII shorter than spI; leg I femur length: carapace width ratio, 1.93—2.21; leg I tibia comprising 34—37 articles, tarsus comprising 70 or 71 articles; leg IV distitibia with 23 or 24 trichobothria.

Phrynus guarionexi sp. nov. is sympatric with *P. longipes* at the type locality. Although there are several similarities, the two species differ markedly in several respects. The carapace and pedipalps are less infuscate in *P. guarionexi* sp. nov., than in sympatric specimens of *P. longipes* (Figs. 1A-C, F, 2). The cuticle is covered with less cerotegument in *P. guarionexi* sp. nov. than *P. longipes*; in sympatric

P. longipes, larger amounts of cerotegument secretion form white deposits on cuticles, producing a tessellate appearance on the opisthosomal tergites in many specimens (Fig. 1F). Unlike in *P. guarionexi* sp. nov., the carapace frontal process of both sexes is not visible in dorsal aspect, in *P. longipes* (Fig. 8A–F; Table 6). The female gonopods of *P. guarionexi* sp. nov. resemble the gonopods of *P. longipes* (Fig. 11; Table 6). The spine counts and granulation of the pedipalps of *P. guarionexi* sp. nov. resemble those of *P. longipes* (Figs. 9 and 10) but the prolateral surface of the tibia is smooth with few setiferous tubercles in *P. longipes* (Table 6). The ratios between the lengths of the pedipalp patella dorsal spines P4: P3 distinguish

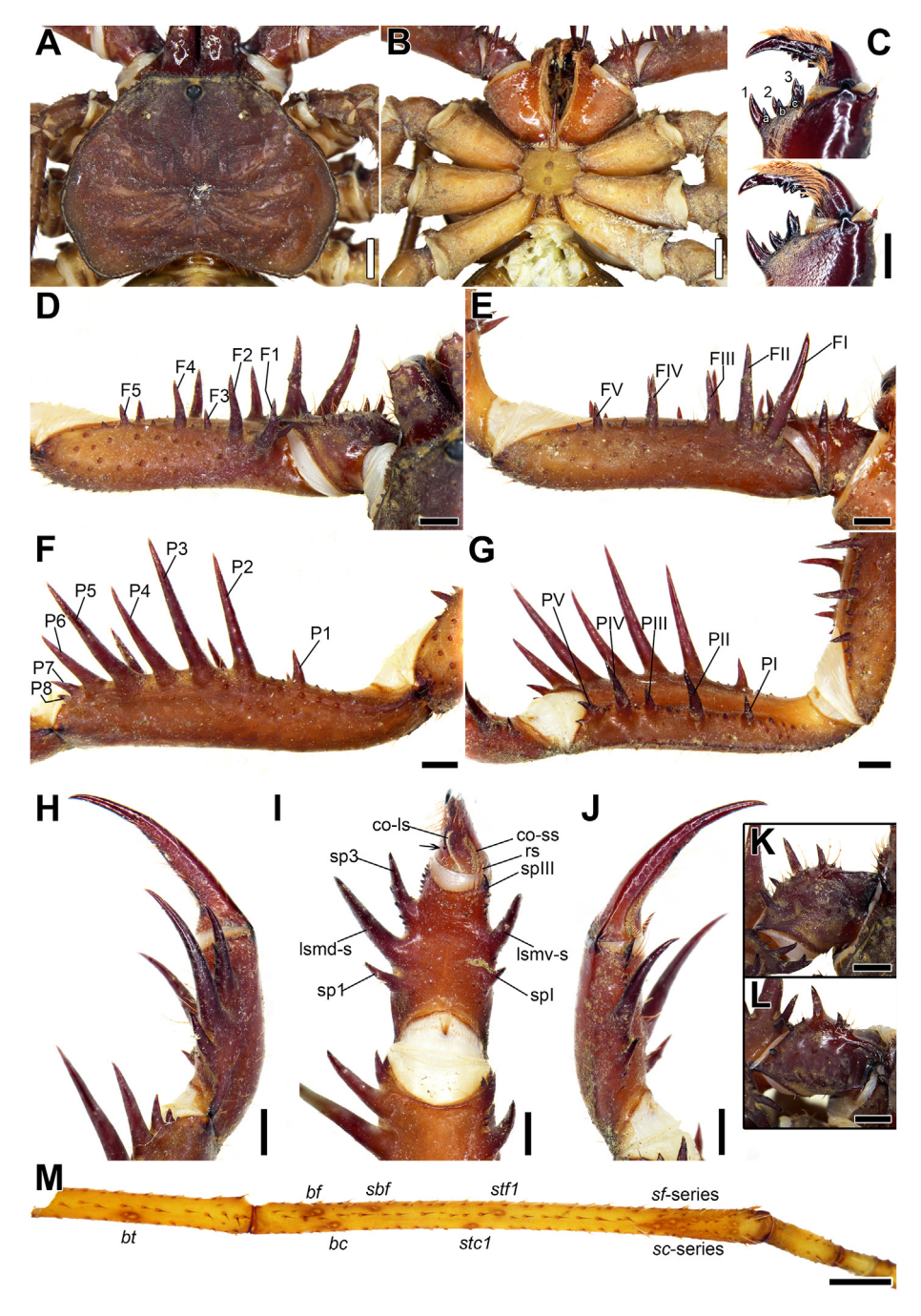


Fig. 7. Phrynus guarionexi sp. nov., holotype 9 (NHMW 29647) (A, B, D—M) and paratype 3 (NHMW 29648) (C), morphology. A. Carapace, dorsal aspect. B. Sternum, ventral aspect. C. Cheliceral dentition (dense setae at cheliceral base removed), prolateral (lower) and retrolateral (upper) aspects. D, E. Sinistral pedipalp trochanter and femur, dorsal (D) and ventral (E) aspects. F, G. Sinistral pedipalp patella, dorsal (F) and ventral (G) aspects. H—J. Sinistral pedipalp tibia and tarsus (and claw), prodorsal (H), prolateral (I), and proventral (J) aspects. K. Sinistral pedipalp trochanter, prolateral aspect. L. Dextral pedipalp trochanter, prolateral aspect. M. Leg IV basitibia and distitibia, prolateral aspect, illustrating number and arrangement of trichobothria; single tubercle on prodorsal surface of pedipalp tarsus in I indicated with arrow. Scale bars: 2 mm (A, B), 1 mm (C—M).

the two sympatric species and do not overlap between P. guarionexi sp. nov. ($4 \ \delta \delta$: carapace width, 8.55-12.7, length P4: P3, 0.76-0.80; \$\$: carapace width, 12-12.2 mm, length P4: P3, 0.76-0.79) and similarly sized ($7 \ \delta \delta$: carapace width, 9.1-12.9, length P4: P3, 0.57-0.66; $7 \ \$\$$: carapace width, 9.4-10.8 mm, length P4: P3, 0.54-0.66) and larger P. longipes ($3 \ \delta \delta$: carapace width, 13.1-15.5, length P4: P3, 0.55-0.58; $4 \ \$\$$: carapace width, 13.4-15.1 mm, length P4: P3, 0.51-0.58) (Fig. $5B: Table \ 4$).

The trichobothrial counts of the leg IV distitibia vary from 23 to 24 in *P. guarionexi* sp. nov., but from 33 to 37 (n = 7) in *P. longipes*: 33–35 (n = 3) in the sympatric population at Monseñor Nouel (NHMW 29651, 29652); 33 or 34 (n = 2) at Samaná (NHMW 29660); and 36 or 37 (n = 2) at La Altagracia (NHMW 29664) (Fig. S4GH; Table 7).

Description: Based on holotype ♀ (NHMW 29647), unless stated otherwise. Variation described in paratypes where applicable.

Color: Carapace, opisthosoma, and trochanter and femur of walking legs brownish red in adults, greyish in juveniles; pedipalps and walking leg segments distal of femur dark reddish in adults, bright red in juveniles (Fig. 1A—C). Cuticle generally not covered by large amounts of cerotegument.

Carapace: Width 1.34 times greater than length (Fig. 7A). Dorsal surface densely covered with coarse setiferous tubercles; anterior margin with fewer setiferous tubercles. Median ocelli well developed, ocular tubercle elevated; lateral ocelli well developed, forming triad. Frontal process small, pointed, visible in frontal aspect but obscure in dorsal aspect (Fig. 7A); weakly developed in paratype ♂ (NHMW 29648) and paratype ♀ (AMMH) (Figs. 8A−C, S4A).

Sternum: Unsclerotized surface with three small, sclerotized sternites bearing setae (Fig. 7B). First sternite (tritosternum) elongated with paired subapical setae, tip of tritosternum broadly projecting between pedipalp coxae; second and third sternites small, oval to circular, each bearing small setae. Pedipalp gnathocoxa, ventral surface with dense vestiture of narrow, reddish setae near small white mesal surface.

Genitalia: Female gonopods evenly sclerotized, with two claw-like appendages (Fig. 11A, C, E), cuspid, rectilinear with rounded, uncurved tip, and base much wider than apex. Male genitalia covered ventrally by genital operculum (Fig. 12A, C); operculum bearing several setae along anterior margin; LoL1 and LoL2 blunt, LoL2 two-thirds length of LoL1; PI small, blunt but prominent; LaM large, cuspid; LoD large, partly sclerotized with blunt but pointed apex.

Chelicerae: Surfaces granular, finely and densely setose, with many setiferous tubercles (Fig. 7C). Prolateral row of teeth comprising three cuspid denticles (1-3); dorsalmost tooth (proximal: 1) largest; ventralmost tooth (distal: 3) bicuspid, dorsal cusp largest; retrolateral row with three teeth (a-c) cuspid (1>3>2>a=b>c); claw (moveable finger) with four prominent teeth.

Pedipalps: No obvious secondary sexual dimorphism in pedipalp length between males and females (Figs. 7 and 10). Pedipalp surfaces coarsely tuberculate. Trochanter prodorsal surface with row of four small spines, all setiferous (Fig. 7D, E, K, L); proventral surface with three large spines and several smaller spinelets, interspersed with setiferous tubercles. Femur with five major dorsal spines (Fig. 7D, E), F2 largest, posterior to F1, additional small spine sharing same base with F1 (holotype ♀ only), F1 with additional subsidiary spine near apex (F2 > F4 > F1 > F5 > F3), interspersed with several small spines; five major ventral spines, FI largest (FI > FII > FIV > FV), interspersed with several small spines. Patella with eight major dorsal spines (Fig. 7F, G), P3 largest (P3 > P5 > P2 > P4 > P6 > P1 > P7 > P8), anterior of P8, situated between P1 and P2, and proximal to P1, interspersed with small spinelets; P3 length: patella width ratio, 1.38-1.86 (n = 7) (Table 2); length P2: P3, 0.85-0.9 (n = 7); length P4: P3, 0.76-0.8(n = 7); length P5: P3, 0.83–0.92 (n = 7); length P6: P3, 0.51–0.54 (n = 7) (Table 4); five major ventral spines, PIV largest (PIV > PII > PIII > PV > PI), interspersed with one or more small spinelets, and additional small spinelet distal to PV. Tibia prodorsal margin with three large spines submedially (Fig. 7H. I), sp2 (= lsmd-s) largest, sp3 with row of small spinelets on proximal margin, row of small spinelets distal to sp3 (lsmd-s > sp3 > sp1); proventral margin with three large spines, spII (lsmv-s) largest, one spinelet at base of spIII; row of small spinelets distal to lsmv-s, distal margin with three apically thickened setae (rs) adjacent to spIII; prolateral surface granular with many setiferous tubercles (Figs. 7I and 9A, B). Tarsus spinose with well-developed cleaning organ (Fig. 7H–J) comprising short row of setae (co-ss) dorsally and long row of setae (co-ls) ventrally, with small tubercle on ventral surface near co-ls; inconspicuous spine on prodorsal surface. Claw not separated from tarsus (Fig. 7H-J).

Legs: Dextral and sinistral antenniform legs (leg I) with 37/34 tibial and 71/70 tarsal articles, respectively (holotype $\mathfrak P$). Leg I femur length: carapace width ratio, 1.98-2.11 ($n_{\mathfrak F}=3$) and 1.93-2.21 ($n_{\mathfrak P}=3$) (Table 2). Walking legs slightly elongated; leg IV, basitibia comprising three articles, third segment with single

Table 6
Comparison of form and shape of carapace frontal process, surface shape and setiferous tubercles on prolateral surface of pedipalp tibia, and female genital sclerite morphology among whip spiders of *Phrynus* Lamarck, 1801 group B (Quintero 1981). Character: Frontal process (\$\delta/\varphi\$): concealed (0), present but weakly developed (1), present and strongly developed (2). Surface shape: smooth (0), granular (1); setiferous tubercles: few (0), many (1). Female genital sclerite length: short (0), intermediate long (1), long (2); width of base vs tip: base slightly wider (0), base much wider (1); form: rectilinear (0), acuminate (1); tip curvature: straight (0), curved (1), blunt (2). See Fig. 8 for illustration. Data from Seiter & Lanner (2017)¹; Chirivi-Joya (2017)²; Harvey (2002)³; Colmenares García and Villarreal (2008)⁴; Armas and Angarita (2008)⁵. Pio Colmenares (pers. commun.) regarding *Phrynus araya* Colmenares García and Villarreal, 2008 indicated with asterisk; n.d. = not described in original publication; *Phrynus tessellatus* (Pocock, 1894) illustrated by Seiter & Lanner (2017) = *Phrynus calypso* Chirivi-Joya, 2017 (Chirivi-Joya 2017).

| | Carapace | Pedipalp tibia | | Female genital sclerite | | | |
|----------------|--|-------------------|----------------------|-------------------------|----------------------|---------|----------------|
| | Frontal process | Surface shape | Setiferous tubercles | Length | Width of base vs tip | Form | Tip curvature |
| P. araya | 0 (♂)*; 0 or 1 (♀); 0 ⁴ | n.d. ⁴ | n.d. ⁴ | 24 | 04 | 0^{4} | 14 |
| P. calypso | 1 $(3)^1$; 2 (9) ; pointed, n.d. ² | 1 | 1 | 1 | 1 | 1 | 1 |
| P. exsul | $0 (\eth)^3; 0 (\Rho);$ | 1 | 1 | 0 | 1 | 1 | 1 |
| P. goesii | 1 or 2 (♂, ♀); broad, blunt and triangular | 0 | 1 | 0 | 1 | 0 | 0 |
| P. guarionexi | 1 (♂); 1–2 (♀); pointed | 1 | 1 | 1 | 1 | 0 | 0 |
| P. longipes | 0 (♂, ♀) | 0 | 0 | 0 | 1 | 0 | 0 |
| P. panche | n.d. ⁵ | n.d. ⁵ | n.d. ⁵ | 2 ⁵ | 0^{5} | 0^{5} | 1 ⁵ |
| P. pinarensis | 2 (♂, ♀); pointed | 0 | 0 | 0 | 0 | 1 | 2 |
| P. pulchripes | $0 (3)^2$; 0 or 1 (\mathfrak{P}); pointed | 1 | 1 | 0 | 1 | 1 | 1 |
| P. tessellatus | ? (♂); 2 (♀); pointed | 1 | 1 | 1 | 0 | 1 | 1 |

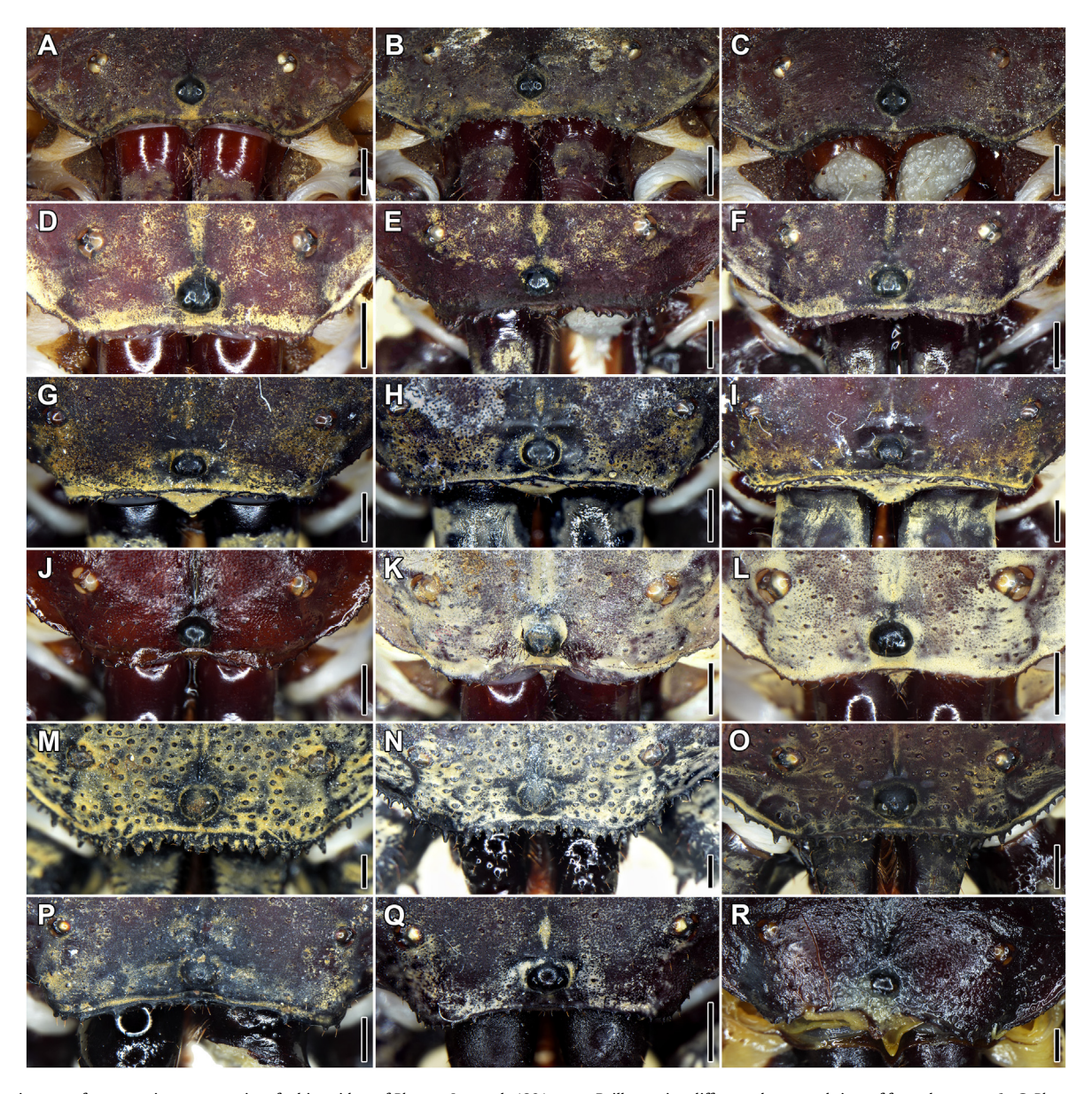


Fig. 8. Anterior part of carapace in seven species of whip spiders of *Phrynus* Lamarck, 1801 group B, illustrating different shapes and sizes of frontal process. A—C. *Phrynus guarionexi* sp. now, A. holotype ♀ (NHMW 29647), B. paratype ♀ (NHMW 29648), C. paratype ♂ (NHMW 29648), Monseñor Nouel, D. Dominican Republic (D.R.), D—F *Phrynus longipes* (Pocock, 1894), D. ♀ (NHMW 29651), F. ♂ (NHMW 29651), F. ♂ (NHMW 29651), Monseñor Nouel, D.R. G—I. *Phrynus goesii* Thorell, 1889, G. ♀, H, L. ♂ (NHMW 28528), St. Maartin, Netherlands Antilles. J—L. *Phrynus pinarensis* Franganillo, 1930, J. ♀ (NHMW 27634), K. ♀ (NHMW 29740), L. ♂ (NHMW 27634), Pinar del Río, Cuba. M—O. *Phrynus exsul Harvey*, 2003, M. ♀ (NHMW 29684), N. O. ♂ (NHMW 29684), East Nusa Tenggara, Indonesia. P. Q. *Phrynus pulchripes* (Pocock, 1894), ♂ (NHMW 27632), Nueva Esparta, Venezuela. R. *Phrynus tessellatus* (Pocock, 1894), ♀ (NHMW 1449), St. Lucia. Scale bars: 1 mm.

trichobothrium bt (basitibial); leg IV, distitibia total length 8.4 mm, with 24 and 23 trichobothria in holotype \mathfrak{P} (Fig. 7M) and paratypes, respectively (Fig. S4G; Table 7), tarsi with slight transverse line, arolium absent in adult.

Measurements (mm): Holotype $\$ (NHMW 29647): Carapace: length, 9.1; width, 12.2. Pedipalp length: femur, 8.4; patella, 9.97; tibia, 4.8; tarsus + claw, 4.8. Leg length: II, 48.8; III, 55.4; IV, 50.6. Paratype ♂ (NHMW 29648): Carapace: length, 9.9; width, 12.7. Pedipalp length: femur, 8.7; patella, 10.54; tibia, 5.0; tarsus + claw, 4.8. Leg length: II, 49.6; III, 55.7; IV, 51.

Distribution: Known only from the type locality in Monseñor Nouel Province, Dominican Republic (Fig. 2).

Natural History: The specimens comprising the type series were collected underneath logs and stones, partially buried in the soil, and in part densely covered with wet and dry leaf litter, near a

small watercourse (Seiter et al., 2018). Two other whip spider species were sympatric at the same locality, i.e., the charinid, *Charinus magua*, and the phrynid, *P. longipes*.

4. Discussion

In the present study, landmark-based morphometrics were used to explore the morphospace of the retrolateral surface and dorsal spination of the pedipalp patella among the species of *Phrynus* group B. New characters for whip spider species delimitation and diagnosis were identified and employed alongside traditional meristic and qualitative characters in the description of *P. guarionexi* sp. nov., offering an example of their potential utility for whip spider taxonomy.



Fig. 9. Prolateral surface of pedipalp tibia in seven species of whip spiders of *Phrynus* Lamarck, 1801 group B. A. *Phrynus guarionexi* sp. nov., holotype ♀ (NHMW 29647), Monseñor Nouel, Dominican Republic (D.R.); rectangle indicates area illustrated in B—H. B. *Phrynus guarionexi* sp. nov., paratype ♂ (NHMW 29648). C. *Phrynus longipes* (Pocock, 1894), ♂ (NHMW 29651), Monseñor Nouel, D.R. D. *Phrynus tessellatus* (Pocock, 1894), ♀ (NHMW 1449), St. Lucia. E. *Phrynus pulchripes* (Pocock, 1894), ♂ (NHMW 27632), Nueva Esparta, Venezuela. F. *Phrynus pinarensis* Franganillo, 1930, ♂ (NHMW 27634), Pinar del Río, Cuba. G. *Phrynus goesii* Thorell, 1889, ♂ (NHMW 28528), St. Maartin, Netherlands Antilles. H. *Phrynus exsul* Harvey, 2003, ♂ (NHMW 29684), East Nusa Tenggara, Indonesia. Arrows indicate setiferous tubercles. Scale bars: 1 mm.

In the most recent revision of the genus *Phrynus* (Quintero 1981 1983), the description of dorsal pedipalp spines as longer or shorter than one another permitted adequate separation of the five known species of *Phrynus* group B. The number of species in the group has since doubled, including *P. guarionexi* sp. nov. The lengths of the dorsal spines on the pedipalp patella follow the same order, i.e., P3 > P5 > P2 > P4 > P6 > P1, in eight of the ten species, providing no means to distinguish among them. Further, although pedipalp patella lengths and widths have been recorded, their use in species delimitation remained underexplored. The geometric

morphometrics analyses presented here demonstrate that, at least among the *Phrynus* species of group B, the shapes of the retrolateral surface of the pedipalp patella and its dorsal spines contain sufficient information to cluster specimens according to species when plotting the first and second principal components. Although overlap was observed between adjacent species clusters, each species can be distinguished from several others.

Pedipalp patellae exhibit large differences in their relative lengths and the relationship between dorsal spine length and patella width, reflecting the perceived slenderness or stoutness of the

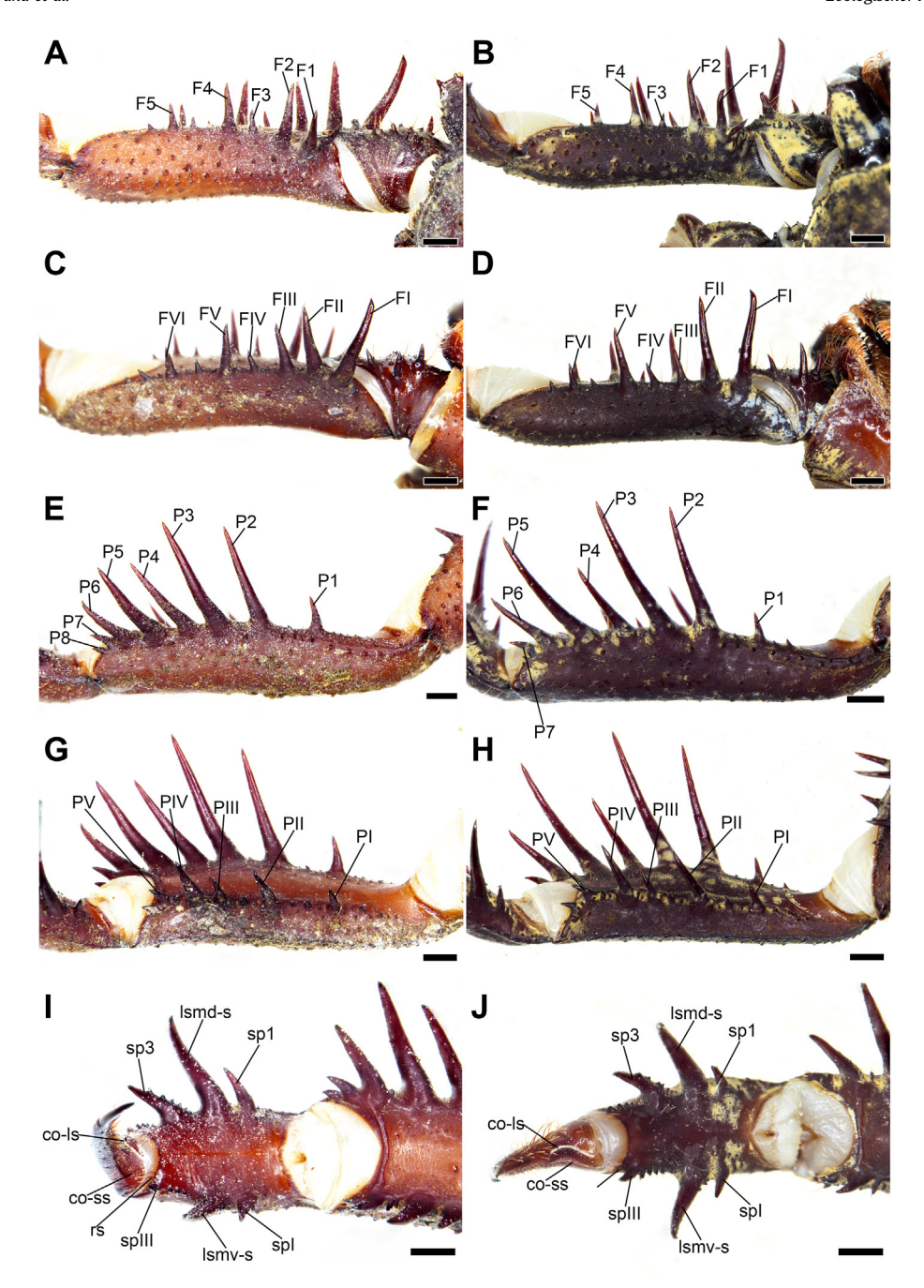


Fig. 10. Phrynus guarionexi sp. nov., paratype & (NHMW 29648), Monseñor Nouel, Dominican Republic (D.R.) (A, C, E, G, I) and Phrynus longipes (Pocock, 1894), & (NHMW 29651), Monseñor Nouel, D.R. (B, D, F, H, J), sinistral pedipalp segments. A—D. Trochanter and femur, dorsal (A, B) and ventral (C, D) aspects. E—H. Patella, dorsal (E, F) and ventral (G, H) aspects. I, J. Distal part of tibia, tarsus and claw, prolateral aspect. Scale bars: 1 mm.

pedipalps among the species of *Phrynus* group B. Intraspecific differences among these morphometric ratios were found to be similar to those observed when comparing the relative length of the leg I femur, a useful character for diagnosing species of *Phrynus* (Quintero 1981 1983). Compared to the pedipalps, the leg I femur is more fragile and more likely to be missing in museum specimens. The pedipalp patella relative length or the relationship between pedipalp patella dorsal spine length and patella width could thus be used instead. It is noteworthy that, at least in some species, these three morphometric ratios change allometrically. In the dataset presented here, this was especially obvious in *P. longipes*, a species in which larger specimens also exhibited sexual dimorphism. Although adult specimens of differing sizes were pooled in the

analysis, it is expected that, as data accumulate, a more fine-scaled comparison among species of similar size will reveal additional interspecific differences.

In contrast to the pedipalp patella relative length and the relationship between patella spine P3 length and patella width, pedipalp patella dorsal spine length ratios were largely constant between sexes and among specimens of variable size, enhancing their potential for broad application to species delimitation. The analyses confirm that *P. calypso*, *P. exsul*, *P. longipes* and *P. tessellatus* share the same spine length formula (P3 > P5 > P2 > P4 > P6 > P1), most common in the species of *Phrynus* group B, and that the spine formulas of *P. goesii* (P5 > P3 > P2 > P4 > P6 > P1) and *P. pinarensis* (P3 > P5 > P4 > P6 > P2 > P1) differ from the other species.

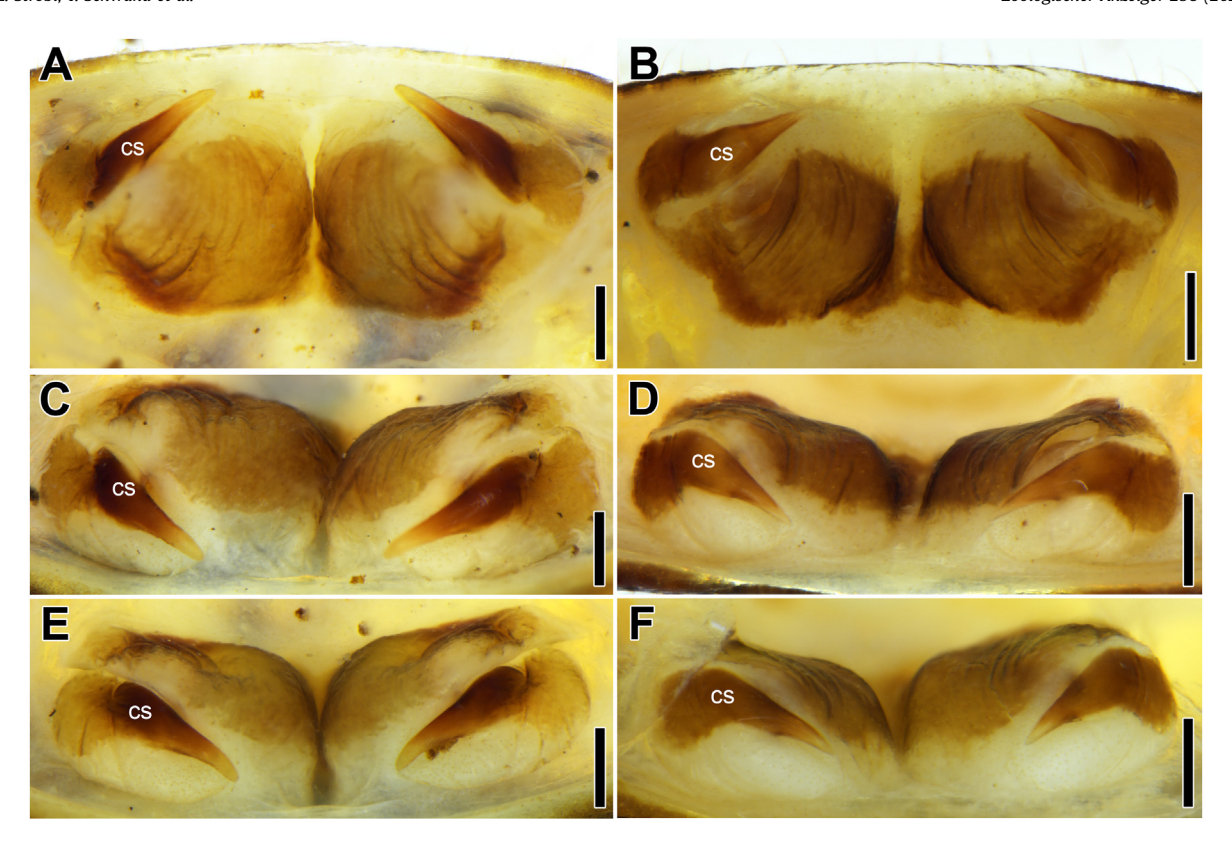


Fig. 11. *Phrynus guarionexi* sp. nov., paratype ♀ (NHMW 29648) (**A, C**) and holotype ♀ (NHMW 29647) (**E**), Monseñor Nouel, Dominican Republic (D.R.), and *Phrynus longipes* (Pocock, 1894), ♀ (NHMW 29652), Monseñor Nouel, D.R. (**B, D**), and ♀ (NHMW 29660), Samaná, D.R. (**F**), genitalia, dorsal (**A, B**) and posterior (**C**—**F**) aspects. Scale bars: 0.5 mm.

Table 7
Comparison of number of teeth on retrolateral margin of chelicera, number of leg I tibial and tarsal articles, and number of trichobothria on distitibia of leg IV among whip spiders of *Phrynus* Lamarck, 1801 group B (Quintero 1981). Data from Seiter & Lanner (2017)¹; Quintero (1981)²; Chirivi-Joya (2017)³; Harvey (2002)⁴; Colmenares García and Villarreal (2008)⁵. Armas and Angarita (2008)⁶. Pio Colmenares (pers. commun.) regarding *Phrynus araya* Colmenares García and Villarreal, 2008 indicated with asterisk; n.d. = not described in original publication. Chirivi-Joya (2017) indicated in text two retrolateral teeth plus carina, whereas in corresponding figure three are visible for *Phrynus calypso* Chirivi-Joya, 2017 (Chirivi-Joya 2017: 361, Fig. 3F), see discussion; *Phrynus tessellatus* (Pocock, 1894) illustrated in Seiter & Lanner (2017) = *Phrynus calypso* (Chirivi-Joya 2017; number of leg IV distitibia trichobothria in *Phrynus araya* counted from illustration in Colmenares García and Villarreal (2008).

| | Number of teeth on retrolateral margin of chelicera | Number of leg I tibial/tarsal articles | Number of leg IV distitibia trichobothria |
|----------------|---|--|---|
| P. araya | 2* | 31-33/> 67 ⁵ | 26 ⁵ |
| P. calypso | 3 (2) ^{1,3} | 31/66 (n=2) | 23 ¹ |
| P. exsul | 2^4 | 31-34/64-66 ($n=3$) | 36 ⁴ |
| P. goesii | 3 | 31-32/66 (n=3) | 21-23 (n=4) |
| P. guarionexi | 3 | 34-37/70-71 (n=4) | 23-24 (n=4) |
| P. longipes | 3 | 35-38/74-75 (n=4) | 33-37 (n=7) |
| P. panche | 2^6 | 30/62 ⁶ | n.d. ⁶ |
| P. pinarensis | 1 | 35-38/64-70 (n=2) | 39-42 (n=2) |
| P. pulchripes | $2^{2,3}$ | 31-32/65-66 $(n=2)$ | 24 (n = 2) |
| P. tessellatus | 3 | 35/n.d. (n=1) | 25 (n = 1) |

Importantly, although *P. guarionexi* sp. nov. presents the same spine length formula (P3 > P5 > P2 > P4 > P6 > P1) as most species of *Phrynus* group B, the dorsal spine length ratios P4: P3 and P6: P3 alone suffice to distinguish the species from all others investigated.

Increased use of morphometric characters in the description of whip spider species and the investigation of differences among populations of putative conspecifics may reveal that these morphologically conservative arachnids are more variable and/or diverse than previously assumed. For example, morphometrics permitted the delimination between populations of *Heterophrynus boterorum* Giupponi & Kury, 2013 and *Phrynus barbadensis* (Pocock, 1893) (González and Morales Álvarez, 1986; Torres et al., 2018; Vásquez et al., 2019), albeit to a variable degree. Widespread whip spider species, such as *P. longipes*, may represent species complexes

on more detailed examination, with a broader set of characters including morphometrics.

The diagnosis presented for *P. guarionexi* sp. nov., which combines traditional characters with new morphometric characters, permits this species to be separated from all other congeners. New morphological data concerning the frontal process of the carapace and the prolateral surface of the pedipalp tibia, identified during the present investigation, add to other characters allowing species delimitation in *Phrynus* group B. The frontal process varies intraspecifically, as it appears to be sexually dimorphic and allometric in most species. This character must therefore be applied cautiously when comparing small samples of closely related species. It has been established that the number of teeth on the retrolateral margin of the chelicera ranges from one

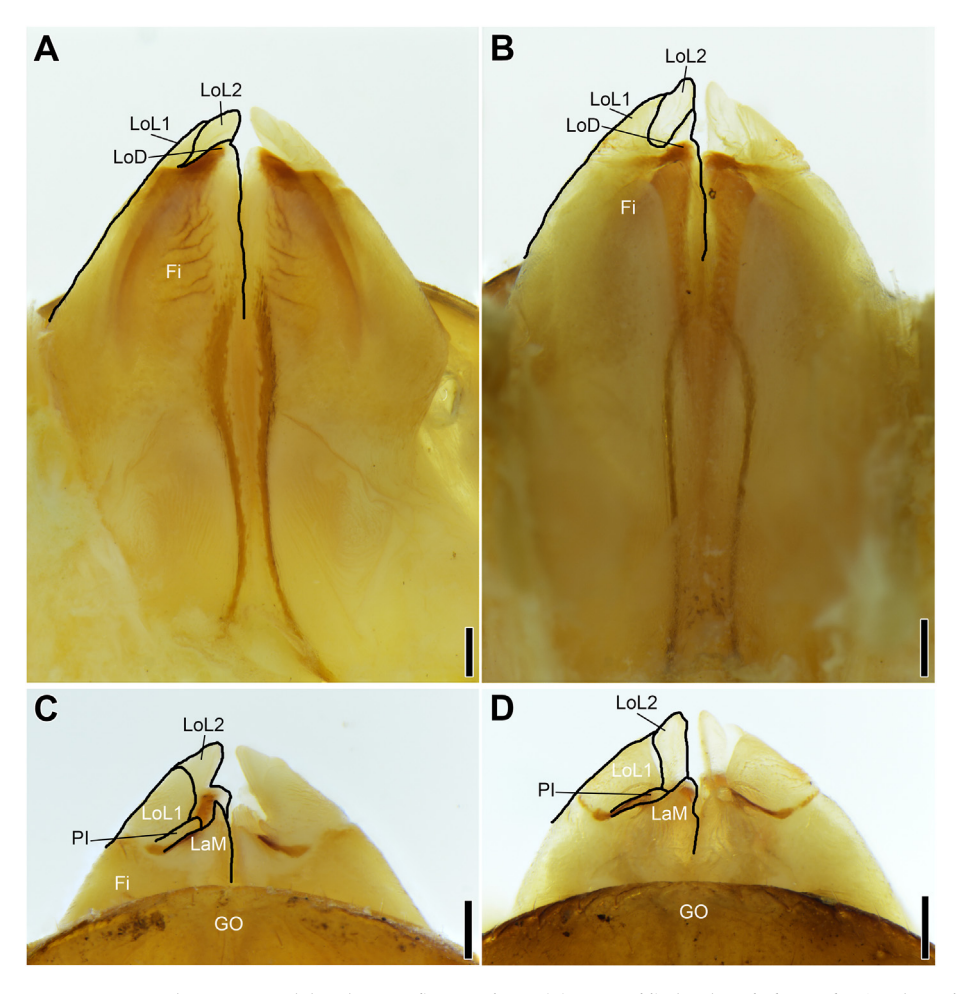


Fig. 12. Phrynus guarionexi sp. nov., paratype & (NHMW 29650) (A, C), Monseñor Nouel, Dominican Republic (D.R.), and Phrynus longipes (Pocock, 1894), & (NHMW 29651), Monseñor Nouel, D.R. (B, D), male gonopods, dorsal (A, B) and ventral (C, D) aspects. Scale bars: 0.25 mm.

to three in the species of *Phrynus* group B. Differences in interpretation by various authors should be noted. For example, Chirivi-Joya (2017) reported two retrolateral teeth plus a keel (carina) in *P. calypso*, a state that may also be interpreted as three teeth.

The presence or absence of a small, inconspicuous spine on the prodorsal surface of the pedipalp tarsus was used by Quintero (1983) to support basal dichotomies in *Phrynus* and *Paraphrynus*, in which some species also exhibit the spine. The species in which the spine is present were termed "group B" in both genera. However, it appears that the classification distinguishing the genera *Phrynus* and *Paraphrynus* based on the dorsal pedipalp patella spination may be artificial. For example, the cerotegument structure of *P. guarionexi* sp. nov. is markedly different from other congeners, more closely resembling two Cuban whip spiders, *Paraphrynus robustus* (Franganillo 1931) and *Paraphrynus viridiceps* (Pocock, 1894) (Wolff et al., 2016; Seiter et al., 2022), both of which also exhibit an inconspicuous spine on the pedipalp tarsus (Quintero 1983).

Author contributions

M.S. and F.D.S. conceived the study; M.S. and L.S. imaged the material; F.D.S performed the landmark-based morphometric analysis; T.S. performed electron microscopy; M.S and F.D.S. processed data, conducted analyses, and prepared the figures; M.S. and F.D.S. interpreted the results; M.S. and F.D.S. wrote the first draft of the manuscript; and T.S., L.S. and L.P. revised the manuscript.

Declaration of competing interest

The authors declare that they have no known competing financial interests or personal relationships that could have appeared to influence the work reported in this paper.

Acknowledgements

M.S. and L.P. were supported by U.S. National Science Foundation grant DEB 2003382 to L.P. The authors thank Rolando Teruel Ochoa, Cuba, and Johannes Nigl, Austria, for assistance in the field; the Departamento de Investigaciones de la Subsecretaria de Areas Protegidas y Biodiversidad, Government of the Dominican Republic, for permission to collect and export arachnids; Stephan Puchegger and the Faculty Center for Nano Structure Research at the University of Vienna for access to the Zeiss Supra55VP electron microscope; Pio Colmenares (AMNH) and Danniella Sherwood (BMNH) for imaging specimens and other assistance in the collections; and two anonymous reviewers for helpful comments on the manuscript.

Appendix A. Supplementary data

Supplementary data to this article can be found online at https://doi.org/10.1016/j.jcz.2022.02.004. Images used for landmark placement, the resulting .tps file, and the R script used for the analysis are deposited in the Dryad Digital Repository (https://doi.org/10.5061/dryad.k0p2ngf9z).

References

- Adams, D., Collyer, M., Kaliontzopoulou, A., Baken, E., 2021. Geomorph: Software for Geometric Morphometric Analyses. R package version 4.0. https://cran.r-project.org/package=geomorph.
- Armas, L.F. de, Calvo, A.Á., 2001. Dos nuevos amblipígidos de Cuba, con nuevos sinónomos y registros (Arachnida: Amblypygi). An. Esc. Nac. Cien. Biol. (Mex.) 46, 289–303.
- Armas, L.F. de, 2006. Sinopsis de los amblipígidos antillanos (Arachnida: Amblypygi). Bol. Soc. Entomol. Aragon. 38, 223–245.
- Armas, L.F. de, Angarita, A.A., 2008. Nueva especie de *Phrynus* Lamarck, 1801 (Amblypygi: Phrynidae) de Colombia. Bol. Soc. Entomol. Aragon. 43, 25–28.
- Baken, E., Collyer, M., Kaliontzopoulou, A., Adams, D., 2021. gmShiny and geomorph v4.0: new graphical interface and enhanced analytics for a comprehensive morphometric experience. Methods Ecol. Evol. 12, 2355–2363.
- Chirivi-Joya, D., 2017. A new species of *Phrynus* Lamarck, 1801 (Arachnida: Amblypygi), from Trinidad and Tobago, and Venezuela, with a redescription of *Phrynus pulchripes* (Pocock, 1894). Zootaxa 4254, 357–374.
- Chirivi-Joya, D., Moreno-González, J.A., Fagua, G., 2020. Two new species of the whip-spider genus *Heterophrynus* (Arachnida: Amblypygi) with complementary information of four species. Zootaxa 4803, 1–41.
- Colmenares García, P.A., Villarreal, O.M., 2008. Una nueva especie de *Phrynus* Lamarck, 1801 (Amblypygi, Phrynidae) de la Sierra de Perijá, Venezuela. Bol. Soc. Entomol. Aragon. 43, 89–93.
- Esposito, L.A., Bloom, T., Caicedo-Quiroga, L., Alicea-Serrano, A.M., Sánchez-Ruíz, J.A., May-Collado, L.J., Binford, G.J., Agnarsson, I., 2015. Islands within islands: diversification of tailless whip spiders (Amblypygi, Phrynus) in Caribbean caves. Mol. Phylogenet. Evol. 93, 107–117.
- Giupponi, A.P., Kury, A., 2013. Two new species of *Heterophrynus* Pocock, 1894 from Colombia with distribution notes and a new synonymy (Arachnida: Amblypygi: Phrynidae). Zootaxa 3647, 329–342.
- González, E.A., Morales Álvarez, L.D., 1986. Variación morfológica en poblaciones alopátricas de *Heterophrynus* (Arachnida, Amblypygi, Phrynidae), vol. 13. Revista de la Universidad de La Salle, pp. 31–41.
- Harvey, M.S., 2002. The first Old world species of Phrynidae (Amblypygi): *Phrynus exsul* from Indonesia. J. Arachnol. 30, 470–474.
- Harvey, M.S., 2003. Catalogue of the Smaller Arachnid Orders of the World: Amblypygi, Uropygi, Schizomida, Palpigradi, Ricinulei and Solifugae. CSIRO Publishing, Collingwood, Australia, p. 385.
- Harvey, M.S., 2013. Whip Spiders of the World. Western Australian Museum, Perth,, Version 1.0. http://museum.wa.gov.au/catalogues-beta/whip-spiders.
- Harvey, M.S., West, P.L.J., 1998. New species of Charon (Amblypygi, Charontidae) from northern Australia and Christmas Island. J. Arachnol. 26, 273–284.
- Kassambara, A., 2021. rstatix: Pipe-Friendly Framework for Basic Statistical Tests. R package version 0.7.0. https://CRAN.R-project.org/package=rstatix.
- Konietschke, F., Friedrich, S., Brunner, E., Pauly, M., 2021. rankFD: Rank-Based Tests for General Factorial Designs. R package version 0.1.0. https://CRAN.R-project. org/package=rankFD.
- McLean, C.J., Garwood, R.J., Brassy, C.A., 2018. Sexual dimorphism in the arachnid orders. PeerJ 6, e5751.
- McLean, C.J., Garwood, R.J., Brassy, C.A., 2019. Sexual dimorphism in the size and shape of the raptorial pedipalps of giant whip spiders (Arachnida: Amblypygi). J. Zool. 310, 45–54.
- Miranda, G.S. de, Giupponi, A.A.P., Prendini, L., Scharff, N., 2018. *Weygoldtia*, a new genus of Charinidae Quintero, 1986 (Arachnida, Amblypygi) with a reappraisal of the genera in the family. Zool. Anz. 273, 23–32.
- Miranda, G.S. de, Giupponi, A.A.P., Prendini, L., Scharff, N., 2021. Systematic revision of the pantropical whip spider family Charinidae Quintero, 1986 (Arachnida, Amblypygi). Eur. J. Taxon. 772, 1–409.

- Prendini, L., Weygoldt, P., Wheeler, W.C., 2005. Systematics of the *Damon variegatus* group of African whip spiders (Chelicerata: Amblypygi): evidence from behaviour, morphology and DNA. Org. Divers. Evol. 5, 203–236.
- Quintero, D.J., 1981. The amblypygid genus *Phrynus* in the Americas (Amblypygi, Phrynidae). J. Arachnol. 9, 117–166.
- Quintero, D.J., 1983. Revision of the amblypygid spiders of Cuba and their relationships with the Caribbean and continental American amblypygid fauna. Stud. Fauna Curação Other Caribb. Isl. 65, 1–54.
- R Core Team, 2021. R: A language and environment for statistical computing. R Foundation for Statistical Computing, Vienna, Austria. https://www.R-project.org.
- Reveillion, F., Wattier, R., Montuire, S., Carvalho, L.S., Bollache, L., 2020. Cryptic diversity within three South American whip spider species (Arachnida, Amblypygi). Zool. Res. 41. 595–598.
- Rohlf, F.J., 2015. The tps series of software. Hystrix 26, 9–12.
- Schramm, F.D., Valdez-Mondragón, A., Prendini, L., 2021. Volcanism and palaeoclimate change drive diversification of the world's largest whip spider (Amblypygi). Mol. Ecol. 30, 2872–2890.
- Seiter, M., Wolff, J.O., 2017. Stygophrynus orientalis sp. nov. (Amblypygi: Charontidae) from Indonesia with the description of a remarkable spermatophore. Zootaxa 4232, 397–408.
- Seiter, M., Gredler, R., 2020. Review of the reproductive behavior and spermatophore morphology in the whip spider genus *Heterophrynus* Pocock, 1894 (Arachnida, Amblypygi), with description of new data and a new species. Zool. Anz. 287, 1–13.
- Seiter, M., Schramm, F.D., Schwaha, T., 2018. Description of a new *Charinus* species (Amblypygi: Charinidae) from the Monseñor Nouel Province, Dominican Republic. Zootaxa 438, 349–361.
- Seiter, M., Lanner, J., 2017. Description and first record of *Phrynus tessellatus* (Pocock, 1894) (Arachnida: Amblypygi: Phrynidae) from northwestern Trinidad, with the description of its mating behaviour. Arachnology 17, 201–209.
- Seiter, M., Reyes Lerma, A.C., Král, J., Sember, A., Divišová, K., Palacios Vargas, J.G., Colmenares, P.A., Loria, S.F., Prendini, L., 2020. Cryptic diversity in the whip spider genus *Paraphrynus* (Amblypygi: Phrynidae): integrating morphology, karyotype and DNA. Arthropod Syst. Phylo. 78, 265–285.
- Seiter, M., Schwaha, T., Prendini, L., Gorb, S.N., Wolff, J.O., 2022. Cerotegument microstructure of whip spiders (Amblypygi: Euamblypygi Weygoldt, 1996) reveals characters for systematics from family to species level. J. Morphol. https:// doi.org/10.1002/jmor.21452.
- Shultz, J.W., 2007. A phylogenetic analysis of the arachnid orders based on morphological characters. Zool. J. Linn. Soc. 150, 221–265.
- Teruel, R., 2016. The genus *Charinus* Simon, 1892 (Amblypygi: Charinidae) on the island of Hispaniola, Greater Antilles. Rev. Ibér. Aracnol. 28, 3–12.
- Torres, R.A., Atencia, P.L., Liria, J., 2018. Morphogeometric variation in *Phrynus barbadensis* (Pocock, 1893) (Amblypyghi [sic]: Phrynidae) from Colombia. Rev. Soc. Entomol. Argent. 77, 18–23.
- Vásquez, S.P., Chirivi-Joya, D., Garcia Hernández, A.L., Mantilla-Meluk, H., Carrera, J.D.T., 2019. Variación morfológica en *Heterophrynus boterorum* (Arachnida: Amblypygi: Phrynidae). Biota Colomb. 20, 32–45.
- Weygoldt, P., 2000. Whip Spiders. Their Biology, Morphology and Systematics. Apollo Books, Stenstrup, Denmark, p. 163.
- Weygoldt, P., Paulus, H.F., 1979. Untersuchungen zur Morphologie, Taxonomie und Phylogenie der Chelicerata. II Cladogramme und die Entfaltung der Chelicerata. J. Zool. Syst. Evol. Res. 17, 177–200.
- Wolff, J.O., Schwaha, T., Seiter, M., Gorb, S.N., 2016. Whip spiders (Amblypygi) become water-repellent by a colloidal secretion that self-assembles into hierarchical microstructures. Zool. Lett. 2, 1–10.
- Wolff, J.O., Seiter, M., Gorb, S.N., 2017. The water-repellent cerotegument of whipspiders (Arachnida: Amblypygi). Arthropod Struct. Dev. 46, 116–129.